Surveillance of Poisson and Multinomial Processes

Anne Garrett Ryan

Dissertation submitted to the Faculty of the
Virginia Polytechnic Institute and State University
in partial fulfillment of the requirements for the degree of

Doctor of Philosophy
In
Statistics

William H. Woodall, Chair
Jeffrey B. Birch
Dong-Yun Kim
Marion R. Reynolds, Jr.

March 18, 2011
Blacksburg, Virginia

Keywords: Average Run Length, Cumulative Sum Chart, Exponentially Weighted Moving Average Chart, Statistical Process Control

Surveillance of Poisson and Multinomial Processes

Anne Garrett Ryan

ABSTRACT

As time passes, change occurs. With this change comes the need for surveillance. One may be a technician on an assembly line and in need of a surveillance technique to monitor the number of defective components produced. On the other hand, one may be an administrator of a hospital in need of surveillance measures to monitor the number of patient falls in the hospital or to monitor surgical outcomes to detect changes in surgical failure rates. A natural choice for on-going surveillance is the control chart; however, the chart must be constructed in a way that accommodates the situation at hand. Two scenarios involving attribute control charting are investigated here. The first scenario involves Poisson count data where the area of opportunity changes. A modified exponentially weighted moving average (EWMA) chart is proposed to accommodate the varying sample sizes. The performance of this method is compared with the performance for several competing control chart techniques and recommendations are made regarding the best preforming control chart method. This research is a result of joint work with Dr. William H. Woodall (Department of Statistics, Virginia Tech). The second scenario involves monitoring a process where items are classified into more than two categories and the results for these classifications are readily available. A multinomial cumulative sum (CUSUM) chart is proposed to monitor these types of situations. The multinomial CUSUM chart is evaluated through comparisons of performance with competing control chart methods. This research is a result of joint work with Mr. Lee J. Wells (Grado Department of Industrial and Systems Engineering, Virginia Tech) and Dr. William H. Woodall (Department of Statistics, Virginia Tech).

Dedication

To Mom and Dad, for always believing in me.

Acknowledgements

First, and foremost, I would like to thank my advisor, Dr. William H. Woodall, for helping me develop the skills to enjoy and succeed in the field of research. Your guidance, encouragement, and support are greatly appreciated. I also express my gratitude to the remaining members of my committee, Dr. Jeffery B. Birch, Dr. Dong-Yun Kim, and Dr. Marion R. Reynolds, Jr. In addition, I would like to thank my co-author Lee Wells for his contributions to the research involving multinomial processes, Lauren Dufresne for helping me make it through my first year of graduate school, and the faculty, staff, and graduate students in the Virginia Tech Statistics Department for support throughout my graduate career. Finally, I would like to thank my entire family for their love and support. Thank you Mom, Dad, Givens, Linden, Adam, Grandmama Tina, and Catherine. I am truly blessed to have such special people in my life.

Contents

List of Tables

List of Figures

Chapter 1

Introduction

Process monitoring is an essential aspect of industrial quality control and public health surveillance. A useful tool in process monitoring is the control chart. The control chart is used to check for process stability by plotting values of a statistic as a function of time, where the statistic is based on the measurement of the quality characteristic of interest. The control chart can be used to quickly detect process shifts so measures can be taken to correct the process, to estimate process parameters to determine process capability, and to reduce variation in the process (Montgomery (2009)).

Walter A. Shewhart was one of the pioneers in quality control and has been credited with creating the first control chart while working at Bell Telephone Laboratories in the 1920's. These control charts, referred to as Shewhart charts, continue to be powerful process monitoring tools (Shewhart (1939)). The Shewhart charts are especially useful in Phase I monitoring because the charts are able to detect large process shifts quickly. Phase I is a retrospective analysis where the objectives include understanding the process behavior, determining if the process is in statistical control, and establishing control limits to be used in future monitoring of the process. The next phase, Phase II, involves real-time process monitoring that builds on the information learned in Phase I.

While Shewhart charts are useful in Phase I monitoring, different methods have been developed to meet specific Phase II objectives. In Phase II, one of the major objectives is to detect small process shifts quickly. The cumulative sum (CUSUM) chart introduced by Page (1954) and the exponentially weighted moving average (EWMA) chart proposed by Roberts (1959) are two effective techniques for detecting process shifts quickly. Unlike the Shewhart

chart that only takes into account information from the most recent sample observation, EWMA and CUSUM charts accumulate information over time. This allows the EWMA and CUSUM charts to be more sensitive to smaller process shifts. Phase II control charting is the focus of the work in this dissertation.

Control charts are developed to handle both continuous and attribute data. The data studied in this dissertation are attribute data particularly Poisson and multinomial observations. The control charts studied for Poisson count data also must take into account varying sample sizes. Control charting techniques that accommodate varying sample sizes are necessary in both healthcare surveillance and industrial applications. This can be the case when monitoring the number of defective components produced where the number of components sampled varies, or in healthcare where the incidence of infection is being monitored as the population changes over time. In both cases the changing area of opportunity must be taken into account. Chapter 2 discusses control charting for Poisson count data as the area of opportunity changes. In this chapter, we compare the performance for different control charting techniques that have been proposed in literature with the performance for a new EWMA approach. This research is a result of joint work with Dr. William H. Woodall (Department of Statistics, Virginia Tech) and has been published in the *Journal of Quality Technology* (Ryan and Woodall (2010)).

Chapter 3 focuses on control charting methods in a multinomial framework. Suppose one is monitoring post-surgery infection for a hospital. Instead of limiting the variable of interest to whether or not the patient developed the infection, one is interested in when the patient is free of infection, has a minor infection, or has a major infection. This is a situation that requires the use of a multinomial CUSUM chart.

The multinomial CUSUM chart is an extension of the Bernoulli CUSUM chart proposed by Reynolds and Stoumbos (1999). The Bernoulli CUSUM chart can be used to monitor a process that produces a continuous stream of inspection data where the outcome is binary, e.g., conforming and non-conforming. However, suppose one has a process where components can be classified into more than two categories, e.g., conforming, minor non-conforming, and major non-conforming. For these situations, the data now follow a multinomial distribution instead of a Bernoulli distribution.

If the original objective had been to monitor the infection rate where the outcome was binary, either the infection exists or does not exist, then Reynolds and Stoumbos (1999) have

shown that the Bernoulli CUSUM chart is the best monitoring approach. Unlike the competing *p*-chart and binomial CUSUM chart, the data does not have to be aggregated over time for monitoring. The Bernoulli CUSUM approach takes advantage of situations where a continuous stream of inspection data exists. However, when the outcome of interest now has three categories, e.g., free of infection, minor infection, and major infection, the Bernoulli CUSUM chart can no longer incorporate the additional category and a multinomial CUSUM chart is needed.

The performance of the multinomial CUSUM chart is compared to the performance for competing control chart methods. This research is a result of joint work with Mr. Lee J. Wells (Grado Industrial and Systems Engineering Department, Virginia Tech) and Dr. William H. Woodall (Department of Statistics, Virginia Tech) and has been accepted for publication in *JQT* (Ryan et al. (2011)).

The next chapter, Chapter 2, is the manuscript titled, “Control Charts for Poisson Count Data with Varying Sample Sizes.” This is followed by Chapter 3, the manuscript, “Methods for Monitoring Multiple Proportions When Inspecting Continuously.” Finally, Chapter 4 discusses conclusions from the current research and future research ideas.

Chapter 2

Control Charts for Poisson Count Data with Varying Sample Sizes

ANNE G. RYAN and WILLIAM H. WOODALL

Virginia Tech, Blacksburg, VA 24061-0439

Various cumulative sum (CUSUM) and exponentially weighted moving average (EWMA) control charts have been recommended to monitor a process with Poisson count data when the sample size varies. We evaluate the ability of these CUSUM and EWMA methods in detecting increases in the Poisson rate by calculating the steady-state average run length (ARL) performance for the charts. Our simulation study indicates that the CUSUM chart based on the generalized likelihood ratio method is best at monitoring Poisson count data at the out-of-control shift for which it is designed when the sample size varies randomly. We also propose a new EWMA method which has good steady-state ARL performance.

Key Words: Average Run Length; Cumulative Sum Chart; Exponentially Weighted Moving Average Chart; Statistical Process Control.

Ms. Ryan is a Ph.D. candidate in the Department of Statistics. Her e-mail address is agryan@vt.edu.

Dr. Woodall is a Professor in the Department of Statistics. He is a fellow of ASQ. His e-mail address is bwoodall@vt.edu.

Introduction

One area of importance in quality control is detection of change for situations with count data where the area of opportunity (sample size) is not constant over time. Examples of varying sample size are prevalent in the industrial setting. Suppose one examines the number of nonconformities in batches, for example, but the batch size is changing across samples. The varying batch size must be taken into account when constructing the control chart.

Situations with varying sample sizes are also common in healthcare surveillance, as when monitoring the incidence of disease in a changing population or the number of new infections in a hospital. Here the size of the at-risk population could change over time, requiring varying sample sizes. Therefore, steps must be taken to accommodate these changes when monitoring the rates.

A common approach to modeling rates is to use the Poisson distribution. Let $X_1,\ X_2,\ \ldots$ be a sequence of observed counts where $n_1,\ n_2, \ldots$ are the respective sample sizes. We assume that $X_1, X_2\ ,\ \ldots$ are independent Poisson observations and that X_i has an in-control mean of $n_i\lambda_0$ and an out-of-control mean of particular interest $n_i\lambda_1,\ i = 1, 2, \ldots$. We focus on the one-sided case where $\lambda_1 > \lambda_0$.

The Shewhart *u*-chart is one of the most common alternatives at handling such changes in the area of opportunity. The *u*-chart is an attribute chart for Poisson random variables that is a plot of the average number of non-conformities per inspection unit, i.e., $\frac{X_i}{n_i}, i = 1, 2, \ldots, m\ ,$ with upper and lower control limits. The retrospective *u*-chart based on m observations signals when one of the plotted points exceeds the control limits, which are given as

$$UCL_i = \bar{u} + L_u\sqrt{\frac{\bar{u}}{n_i}} \text{ and } LCL_i = \bar{u} - L_u\sqrt{\frac{\bar{u}}{n_i}}\ , i = 1, 2, \ldots, m\ , \quad (1)$$

respectively, where $\bar{u} = \frac{\sum_{i=}^{m} X_i}{\sum_{i=1}^{m} n_i}$. Often $L_u = 3$, resulting in the usual three-sigma limits (Montgomery (2009)). There is no LCL for sample i if $\text{LCL}_\text{i} < 0$.

There are two distinct phases associated with control charting. Phase I is a retrospective analysis of previously taken samples. The objectives include understanding the process behavior, determining if the process is in statistical control, and establishing control limits to be used in future monitoring of the process. The next phase, Phase II, involves real-time process monitoring

that builds on the information learned in Phase I. The u-chart in Equation (1) is a useful tool for Phase I control charting, where m is the number of historical values available.

The control limits for the u-chart during Phase II control charting are

$$UCL_i = \lambda_0 + L_u\sqrt{\frac{\lambda_0}{n_i}} \text{ and } LCL_i = \lambda_0 - L_u\sqrt{\frac{\lambda_0}{n_i}}, i = m+1, m+2, \ldots, \quad (2)$$

where λ_0 is the in-control mean number of non-conformities per inspection unit. Again, there is no LCL at sample i if $\text{LCL}_\text{i} < 0$. The value of λ_0 is estimated from the Phase I analysis in practice, but usually assumed to be a known constant in comparisons of control-chart performance.

While the u-chart can be used to monitor processes with varying sample sizes in both Phase I and Phase II control charting, one drawback is that Shewhart charts are not sensitive to detecting small parameter shifts during Phase II analyses. A major objective is to detect changes in incidence rates as quickly as possible. Therefore, more sensitive charts like the cumulative sum (CUSUM) control charts and exponentially weighted moving average (EWMA) control charts are often utilized during Phase II analyses (Montgomery (2009)).

The task of accounting for varying sampling sizes when using both CUSUM and EWMA charts has been studied by several researchers. Mei et al. (2011) proposed using a CUSUM technique derived from a generalized likelihood-ratio method. Yashchin (1989) and Hawkins and Olwell (1998) previously recommended using this weighted CUSUM statistic, but only Mei et al. (2011) studied the properties of the chart. Mei et al. (2011) also proposed two other adaptations of the CUSUM chart.

Yashchin (1989) modified the CUSUM technique based on the log-likelihood ratio to include a geometric weighting factor that assigns less weight to past observations. Shu et al. (2010) studied the performance of two geometrically weighted CUSUM techniques compared to other weighted CUSUM methods for monitoring with Poisson data when the sample size varies.

Another CUSUM technique, recommended by Rossi et al. (1999) and Rossi et al. (2010), is based on a standardization transformation of the observed counts. We refer to this as the standardized CUSUM chart. They claimed this CUSUM procedure can handle situations, especially in healthcare, where the size of the at-risk population varies over time.

Rather than using CUSUM techniques for fast detection, Dong et al. (2008) advised using EWMA methods. The statistics that are weighted by the EWMA method are the observed counts

divided by the corresponding sample sizes. A similar use of this type of EWMA chart was employed by Martz and Kvam (1996), where both an EWMA chart and a Shewhart chart were used to check for trends or patterns over time. The central idea in both papers is to divide the observed counts by the corresponding sample sizes in order to handle varying sample sizes.

The CUSUM and EWMA techniques are intended to handle changes in sample size, but it is not clear which method is most effective. We answer this question by comparing the different techniques using average run length (ARL) performance. The ARL of a control chart is the average number of points that are plotted before a chart signals. This signal can be a true signal of a shift in the process or a false alarm, meaning the chart signaled when, in fact, there was no shift. The out-of-control ARL (or ARL_1) is the expected number of samples before a shift is detected, while the in-control ARL (or ARL_0) is the expected number of samples before a false alarm. The goal is usually to minimize the ARL_1 value over a range of process shifts while requiring a specified value of ARL_0. The measured ARL values can either be zero-state or steady-state ARL values. Zero-state ARL values are based on sustained shifts in the parameter that occur under the initial startup conditions of the control chart, while steady-state ARL values are based on delayed shifts in the parameter.

The steady-state ARL metric is the best measurement of performance for the comparisons of the various methods considered in our paper. The first reason for using steady-state ARL performance over zero-state ARL performance involves the fact that the EWMA chart has a slight advantage over the CUSUM chart at early stages of monitoring. At the initial stages of monitoring, the variance of the EWMA statistic is smaller, which leads to tighter control limits. As a result, the one-sided EWMA chart has a slight head start over the competing CUSUM charts.

The second, more important, argument against using zero-state ARL analyses is based the idea that the optimal smoothing parameter for the EWMA chart approaches zero when considering zero-state ARL performance. Frisén (2009) stated that many researchers found the optimal smoothing constant for the EWMA chart to be around $r = .2$. However, Frisén and Sonesson (2006) revealed how this “optimal” value was, in fact, not optimal because it was based on the local minimum zero-state ARL_1 value and not the global minimum. The global minimum occurs as r approaches zero, which gives approximately equal weight to all of the observations. This chart design is not reasonable, however, if one wants to detect delayed shifts

in the parameter. In a discussion of Frisén (2009), Knoth (2009) pointed out that this problem with the smoothing constant approaching zero is primarily seen with one-sided EWMA charts, which are the types of EWMA charts compared in our paper. These two concerns associated with using zero-state ARL performance have prompted us to examine steady-state ARL performance.

The CUSUM and EWMA methods are explained in the next section. Then simulation results for steady-state ARL performance are given for the situation where the sample size is fixed in order to lay a foundation for comparisons. This is followed by a section with simulation results where sample sizes vary randomly to evaluate the performance of the proposed methods. Next, simulation results are given for comparisons of ARL performance for Poisson processes with low-counts. An example is given in the following section to illustrate and compare the use of two EWMA charts, the u-chart, and a CUSUM chart. The last section provides our concluding remarks and future research ideas. Additional ARL comparisons are given in the appendix.

Cumulative Sum and Exponentially Weighted Moving-Average Methods

The first method we define is a standardized CUSUM chart for Poisson count data proposed by Rossi et al. (1999) and Rossi et al. (2010). They compared three techniques to transform the Poisson counts into approximately normal random variables. The first transformation is

$$Z_{1,i} = \frac{X_i - n_i\lambda_0}{\sqrt{n_i\lambda_0}}, i = 1, 2, \ldots .$$

This transformation is based on the asymptotic normality of the observed count, X_i, with an approximate in-control mean $n_i\lambda_0$ and approximate standard error $\sqrt{n_i\lambda_0}$. The second transformation is the square-root transformation, i.e.,

$$Z_{2,i} = 2\left(\sqrt{X_i} - \sqrt{n_i\lambda_0}\right), i = 1, 2, \ldots ,$$

with approximate in-control mean and standard error of $\sqrt{n_i\lambda_0}$ and ½, respectively. This normalizing transformation stabilizes the variance. The final transformation is the average (called half-sum) transformation of the previous two transformations. Rossi et al. (1999) recommended using a CUSUM chart with the half-sum standardizing transformation because they found the half-sum transformation produced ARL values closest to the ARL values

estimated by Ewan and Kemp (1960) for a Poisson variate. The recommended half-sum transformation is

$$Z_{3,i} = \frac{X_i - 3n_i\lambda_0 + 2\sqrt{X_i n_i \lambda_0}}{2\sqrt{n_i\lambda_0}}, i = 1, 2, \ldots . \quad (3)$$

The resulting distribution for the transformation in Equation (3) will be approximately normal with an approximate in-control mean of 0 and an approximate standard error of 1. Rossi et al. (1999) then defined the CUSUM statistics as follows:

$$S_i = \max\left(0, S_{i-1} + Z_{3,i} - k\right), i = 1, 2, \ldots ,$$

where the chart signals if $S_i \geq h$. The constant k is referred to as the reference value and it is often chosen to be halfway between the in-control mean and the out-of-control mean. Rossi et al. (1999) recommend using the specified values for ARL_0 and ARL_1 to determine h and k.

In situations where the in-control mean is small, the values for ARL_0 are lower than anticipated when the Rossi et al. (1999) standardized CUSUM chart with the fixed reference value, k, is used as discussed in Rogerson and Yamada (2004) and Höhle and Paul (2008). To resolve these issues Rossi et al. (2010) proposed a standardized CUSUM chart with a varying reference value.

The varying reference value, k_i, is half the value of the out-of-control mean at each sample point. The out-of-control mean when $\lambda = \lambda_1$ is approximately

$$E\left[Z_{3,i}; \lambda_1\right] = \frac{n_i\lambda_1 - 3n_i\lambda_0 + 2n_i\sqrt{\lambda_0\lambda_1}}{2\sqrt{n_i\lambda_0}}, i = 1, 2, \ldots ,$$

with a standard error approximately equal to 1. The varying reference limit becomes

$$k_i = \frac{E\left[Z_{3,i}; \lambda_1\right]}{2}, i = 1, 2, \ldots .$$

For the half-sum transformation in Equation (3), the values of $Z_{3,i}$ and k_i are substituted into the following CUSUM statistic formula:

$$S_{1,i} = \max\left(0, S_{1,i-1} + Z_{3,i} - k_i\right), i = 1, 2, \ldots , \quad (4)$$

where $S_{1,0} = 0$. The chart signals if $S_{1,i} \geq h_1$, where the value h_1 is determined based on the specified value of ARL_0.

The generalized likelihood ratio (GLR) CUSUM method proposed by Yashchin (1989), Hawkins and Olwell (1998), and Mei et al. (2011) is based on the statistics

$$S_{2,i} = \max\left(0, S_{2,i-1} + X_i - \frac{n_i(\lambda_1 - \lambda_0)}{\ln(\lambda_1) - \ln(\lambda_0)}\right), i = 1, 2, \ldots, \quad (5)$$

where $S_{2,0} = 0$. The chart signals if $S_{2,i} \geq h_2$, where the value h_2 is determined based on the specified value of ARL_0. Mei et al. (2011) showed how the construction of the GLR CUSUM statistic is similar to constructing a test of a null hypothesis using the GLR method.

The next two methods we review are two alternative methods proposed by Mei et al. (2011). The first alternative method, referred to as the weighted likelihood ratio (WLR) CUSUM procedure, is based on the statistics

$$S_{3,i} = \max\left(0, S_{3,i-1} + \frac{X_i}{n_i} - \frac{\lambda_1 - \lambda_0}{\ln(\lambda_1) - \ln(\lambda_0)}\right), i = 1, 2, \ldots . \quad (6)$$

The starting value $S_{3,0}$ is 0, and the chart signals if $S_{3,i} \geq h_3$.

Another method proposed by Mei et al. (2011) introduced varying thresholds into the CUSUM statistic in Equation (5) to account for the varying samples sizes. Instead of having a constant decision interval, the threshold method uses the same CUSUM statistics in Equation (5), but signals when $S_{2,i} \geq n_i h_4$. Mei et al. (2011) referred to this method as the adaptive threshold method (ATM).

It is important to notice that the GLR, WLR, and ATM methods are all equivalent when the sample sizes are constant. These methods are then the same as the method proposed by Lucas (1985). Lucas (1985) used Markov chains to calculate the ARL values of CUSUM charts for Poisson count data with fixed sample sizes. Also, Moustakides (1986) proved this method, which is based on a likelihood-ratio approach, to have optimality properties in detecting a change in distribution. However, differences among the procedures arise when the samples sizes vary, and the optimality property may no longer apply.

Mei et al. (2011) explored the GLR, WLR, and ATM methods both theoretically and through a simulation study. They studied cases for which the sample size was either monotonically increasing or monotonically decreasing. They found the performance of the GLR CUSUM chart to be better than that of the WLR CUSUM chart when the sample sizes were decreasing and worse when the sample sizes were increasing. The ATM method seemed to have

the overall best performance because its relative performance did not depend so much on the sample-size pattern. In our simulation study we consider the cases in which the sample sizes vary randomly.

The next procedure to be considered is the EWMA method recommended by both Dong et al. (2008) and Martz and Kvam (1996). The EWMA statistics are

$$Z_i = r\frac{X_i}{n_i} + (1-r)Z_{i-1}, i = 1, 2, \dots, \tag{7}$$

where $Z_0 = \lambda_0$ and $r \in (0,1]$ is the smoothing parameter that determines the weights assigned to past data. More weight is given to past data points as r gets closer to 0, which results in better detection of smaller shifts. However, one concern with making the value of r too small is the inertial effect. As discussed by Woodall and Mahmoud (2005), an adverse inertial effect occurs when the value of the EWMA statistic is on one side of the centerline and the shift in the parameter occurs toward the opposite side of the centerline. Because much weight is given to past data, this can cause a delay in the detection of the shift in the parameter. On the other hand, if r is set to a large value, it can take longer for a small shift to be detected. When $r = 1$, the EWMA chart is equivalent to the Shewhart chart, which is most effective in detection of large shifts. It has been suggested to use values of r in the interval $0.05 \leq r \leq 0.25$ (Montgomery (2009)); however, Dong et al. (2008) suggested using $r = .9$. Martz and Kvam (1996) found the EWMA chart to perform well when $r = .1$, but they also recommended using a Shewhart chart in conjunction with the EWMA chart to detect large shifts.

Dong et al. (2008) explored three different control limit approaches for their EWMA method. Since they were focused on detecting an increase in the incidence rate, they used only upper control limits for the three methods. The first set of upper control limits are based on the exact variances of the EWMA statistics, i.e.,

$$UCL_{1,i} = \lambda_0 + L_1\sqrt{r^2\sum_{j=1}^{i}(1-r)^{2i-2j}\frac{\lambda_0}{n_j}}, i = 1, 2, \dots; \tag{8}$$

the second set of upper control limits is

$$UCL_{2,i} = \lambda_0 + L_2\sqrt{\frac{\lambda_0}{n_0}\frac{r}{2-r}[1-(1-r)^{2i}]}\ i = 1, 2, \dots m; \tag{9}$$

while the third upper control limit, which is based on the asymptotic variance as $i \to \infty$ in Equation (9), is

$$UCL_3 = \lambda_0 + L_3\sqrt{\frac{\lambda_0}{n_0}\frac{r}{2-r}}. \tag{10}$$

The value n_0 is the minimum sample size of all the values of $n_i,\ i = 1, 2, \ldots m$. A signal is given when Z_i exceeds the UCL.

The use of the minimum sample size in the control-limit computations leads to a problem related to the overall objective of the EWMA control chart. Both the EWMA and CUSUM charts were developed as Phase II methods. These charts are effective at monitoring a process that has been operating in control. This means one will not know beforehand the minimum sample size of the entire set of samples because the samples are being taken in real time. Knowledge of the minimum sample size is required to use the EWMA statistics with the UCLs in Equation (9) or Equation (10) as Phase II charts. We index the UCLs in Equation (9) and Equation (10) by $i = 1, 2, \ldots, m$, where m is the number of samples taken in Phase I, to indicate that it seems reasonable to use these methods only in Phase I. We note, however, that the EWMA approach is not appropriate for Phase I since quick detection of a rate increase is no longer an objective.

Martz and Kvam (1996) gave the control limits based on the exact variance but used the EWMA chart only with Phase I data. For their simulation study they considered both equal and unequal sample sizes.

Another issue with the EWMA charts of Dong et al. (2008) is that there is no reflecting lower barrier. They are only interested in detecting an increased rate so they simply remove the LCL. The exclusion of this limit allows the EWMA statistics to take on very small values, which then could lead to serious inertial problems, especially if the value of r is small (Woodall and Mahmoud (2005)). A much better approach is to use a reflecting barrier at $Z_i = \lambda_0$, as proposed by Crowder and Hamilton (1992) in a different context. Martz and Kvam (1996) recommended an EWMA chart that has both upper and lower control limits, but again it seems as if they are using a Phase II method in Phase I.

We propose using a new EWMA method that differs from the EWMA techniques discussed by Dong et al. (2008). Our EWMA chart, which we refer to as the modified EWMA method (EWMA-M), has a lower reflecting barrier at $Z_i = \lambda_0$ and the control limits are based on

the exact variances of the EWMA statistics, as seen in Equation (8). We consider a range of values for the smoothing constant, r, to illustrate the need to select the value of r based on the shift size of interest.

Simulation Results for Constant Sample Size

In this section we summarize the results of a simulation study comparing the steady-state ARL performance of the previously discussed EWMA and CUSUM methods where the sample sizes are fixed, without loss of generality at $n_i = 1$ for $i = 1, 2, \ldots$. This study provided baseline information about the performance of the EWMA and CUSUM methods. We expected that if a method had poor performance when the sample sizes were fixed, then the performance of this method would likely remain poor when the sample sizes were allowed to vary.

One method compared will be referred to as the weighted CUSUM method, which represents the GLR, WLR, and ATM CUSUM methods. Because the sample size is constant, all three of these CUSUM methods, along with the Lucas (1985) CUSUM method, are equivalent. The next technique compared is the standardized CUSUM chart in Equation (4). The last two methods compared are EWMA techniques. One EWMA method, called EWMA-3, has control limits based on the asymptotic variance of the EWMA statistics as seen in Equation (10). The smoothing constant for the EWMA-3 technique is set to $r = .9$, the value recommended in Dong et al. (2008). The second EWMA technique is our new EWMA method, EWMA-M. This chart has control limits in Equation (8), which are based on the exact variances of the EWMA statistics. The smoothing constant takes on values $r = .05, .1, .15, \text{and } .2$, allowing us to choose the best smoothing constant for the parameter shift of interest.

In our simulation study we used 10,000 repetitions to estimate each ARL value. The values of L for the EWMA methods and h for the CUSUM methods used in the steady-state simulation study were determined so that the charts had zero-state ARL_0 values equal to 200. The process was run at an in-control state for 50 samples and then the shift in the parameter occurred. If a simulated chart signaled that the rates had increased during the first 50 samples, then that particular run was discarded and a new set of 50 samples were generated. Table 2.1 contains the different combinations of λ_0 and λ_1 values studied. Other combinations we considered yielded similar conclusions to those obtained with these combinations.

Table 2.1. Combinations of λ_0 and λ_1 Studied Through Simulation

λ_0	λ_1
6	7
6	8
6	9
10	12
10	14
10	18
10	20

Table 2.2 presents the steady-state ARL values for various shifts in the Poisson mean where $\lambda_0 = 10$ and $\lambda_1 = 12$. The weighted CUSUM chart ARL values are slightly less than the standardized CUSUM chart ARL values for small shifts in the mean. Once the mean has shifted to approximately $\lambda = 13$, the standardized CUSUM chart starts to have slightly better performance. Both the weighted and standardized CUSUM charts have considerably better performance for detection of small shifts compared to the EWMA-3 method of Dong et al. (2008). It is not until the mean has undergone a shift to $\lambda = 18$ that the EWMA-3 method begins to have better performance.

The simulation results reveal for small shifts of interest it is best to use the EWMA-M chart with $r = .05$. This EWMA-M chart has better performance compared to all the other EWMA methods for shifts up to $\lambda = 12$. The EWMA-M chart with $r = .05$ also has quicker detection compared to the weighted CUSUM and standardized CUSUM methods for mean shifts of $\lambda = 12$ or less.

The steady-state ARL performance comparison for the case where $\lambda_0 = 10$ and $\lambda_1 = 14$ is shown in Table 2.3. The weighted CUSUM chart slightly outperforms the standardized CUSUM chart for shifts in the mean of $\lambda = 15$ or less. For very small shifts the best chart is the EWMA-M chart with $r = .05$. We will see that the best value of r for the EWMA-M method increases as the mean shift of interest increases. Also notice that the EWMA-3 method with the large smoothing constant does not have quick detection until very large shifts in the mean occur.

Table 2.2. Comparison of ARL Values for $\lambda_0 = 10$ and $\lambda_1 = 12$ with $ARL_0 \approx 200$

λ	$h_2 = 16.33$ Weighted CUSUM	$h_1 = 4.68$ Standardized CUSUM	$L_1 = 2.24$ EWMA-M $(r = .05)$	$L_1 = 2.47$ EWMA-M $(r = .1)$	$L_1 = 2.59$ EWMA-M $(r = .15)$	$L_1 = 2.66$ EWMA-M $(r = .2)$	$L_3 = 2.85$ EWMA-3 $(r = .9)$
10.25	114.65	117.26	115.09	119.80	123.69	126.33	153.17
10.50	71.47	73.31	67.84	73.77	78.43	83.08	118.15
10.75	47.37	49.27	44.78	49.62	54.59	57.65	91.14
11.00	33.36	34.65	31.55	34.67	37.80	41.28	72.28
11.50	19.38	19.93	19.12	20.10	21.62	23.40	46.05
12.00	**13.10**	**13.43**	**13.06**	**13.45**	**14.01**	**14.82**	**31.71**
13.00	7.67	7.66	8.00	7.75	7.66	7.96	16.10
14.00	5.44	5.40	5.81	5.40	5.28	5.30	9.30
15.00	4.27	4.19	4.62	4.15	3.97	3.91	5.96
16.00	3.53	3.49	3.80	3.42	3.21	3.13	4.13
18.00	2.64	2.63	2.91	2.56	2.40	2.30	2.44
20.00	2.16	2.17	2.37	2.08	1.93	1.83	1.72

Table 2.3. Comparison of ARL Values for $\lambda_0 = 10$ and $\lambda_1 = 14$ with $ARL_0 \approx 200$

λ	$h_2 = 10.50$ Weighted CUSUM	$h_1 = 2.95$ Standardized CUSUM	$L_1 = 2.24$ EWMA-M $(r = .05)$	$L_1 = 2.47$ EWMA-M $(r = .1)$	$L_1 = 2.59$ EWMA-M $(r = .15)$	$L_1 = 2.66$ EWMA-M $(r = .2)$	$L_3 = 2.85$ EWMA-3 $(r = .9)$
10.25	131.22	131.86	115.09	119.80	123.69	126.33	153.17
10.50	86.94	88.39	67.84	73.77	78.43	83.08	118.15
10.75	60.88	61.97	44.78	49.62	54.59	57.65	91.14
11.00	43.15	44.73	31.55	34.67	37.80	41.28	72.28
11.50	24.88	25.62	19.12	20.10	21.62	23.40	46.05
12.00	15.41	15.88	13.06	13.45	14.01	14.82	31.71
13.00	8.10	8.30	8.00	7.75	7.66	7.96	16.10
14.00	**5.30**	**5.35**	**5.81**	**5.40**	**5.28**	**5.30**	**9.30**
15.00	3.89	3.91	4.62	4.15	3.97	3.91	5.96
16.00	3.13	3.12	3.80	3.42	3.21	3.13	4.13
18.00	2.28	2.26	2.91	2.56	2.40	2.30	2.44
20.00	1.83	1.84	2.37	2.08	1.93	1.83	1.72

Tables 2.4 and 2.5 present steady-state ARL values where again $\lambda_0 = 10$, but now $\lambda_1 = 18$ and $\lambda_1 = 20$, respectively. With the larger values of λ_1, the steady-state ARL values of the weighted CUSUM methods and the standardized CUSUM methods are very close. The increase in λ_1 also causes a decrease in the difference between the ARL values of the CUSUM methods and the EWMA-3 method, but the CUSUM methods continue to have better detection of smaller shifts. As the shift in the mean increases, the methods tend to perform similarly.

The simulation results in Tables 2.4 and 2.5 illustrate the idea that the value of r for the EWMA-M method should be chosen based on the size of the shift of interest. When one is interested in mean shifts from $\lambda_0 = 10$ to $\lambda_1 = 18$, one should choose $r = .2$. As the size of the shift of interest increases, so too should the value or r.

The case where $\lambda_0 = 10$ and $\lambda_1 = 20$ was the only situation studied by Dong et al. (2008). Our results indicate that the EWMA-3 charts begin to have better performance as the shift in the mean increases. This explains their recommendation of using a smoothing parameter $r = .9$ because EWMA charts with large values of r are known to be effective at detecting large shifts in the Poisson rate. Dong et al.'s (2008) simulation study did not address smaller shifts in the mean or cases with varying sample sizes.

Table 2.4. Comparison of ARL Values for $\lambda_0 = 10$ and $\lambda_1 = 18$ with $ARL_0 \approx 200$

λ	$h_2 = 6.39$ Weighted CUSUM	$h_1 = 1.56$ Standardized CUSUM	$L_1 = 2.24$ EWMA-M ($r = .05$)	$L_1 = 2.47$ EWMA-M ($r = .1$)	$L_1 = 2.59$ EWMA-M ($r = .15$)	$L_1 = 2.66$ EWMA-M ($r = .2$)	$L_3 = 2.85$ EWMA-3 ($r = .9$)
10.25	143.23	143.07	115.09	119.80	123.69	126.33	153.17
10.50	108.24	108.30	67.84	73.77	78.43	83.08	118.15
10.75	79.92	80.28	44.78	49.62	54.59	57.65	91.14
11.00	61.96	62.15	31.55	34.67	37.80	41.28	72.28
11.50	37.72	37.94	19.12	20.10	21.62	23.40	46.05
12.00	24.14	24.45	13.06	13.45	14.01	14.82	31.71
13.00	11.50	11.62	8.00	7.75	7.66	7.96	16.10
14.00	6.63	6.67	5.81	5.40	5.28	5.30	9.30
15.00	4.44	4.47	4.62	4.15	3.97	3.91	5.96
16.00	3.26	3.28	3.80	3.42	3.21	3.13	4.13
18.00	**2.13**	**2.13**	**2.91**	**2.56**	**2.40**	**2.30**	**2.44**
20.00	1.62	1.62	2.37	2.08	1.93	1.83	1.72

Table 2.5. Comparison of ARL Values for $\lambda_0 = 10$ and $\lambda_1 = 20$ with $ARL_0 \approx 200$

λ	$h_2 = 4.95$ Weighted CUSUM	$h_1 = 1.18$ Standardized CUSUM	$L_1 = 2.24$ EWMA-M ($r = .05$)	$L_1 = 2.47$ EWMA-M ($r = .1$)	$L_1 = 2.59$ EWMA-M ($r = .15$)	$L_1 = 2.66$ EWMA-M ($r = .2$)	$L_3 = 2.85$ EWMA-3 ($r = .9$)
10.25	153.94	154.86	115.09	119.80	123.69	126.33	153.17
10.50	117.70	118.58	67.84	73.77	78.43	83.08	118.15
10.75	89.04	89.52	44.78	49.62	54.59	57.65	91.14
11.00	68.95	69.77	31.55	34.67	37.80	41.28	72.28
11.50	42.77	43.39	19.12	20.10	21.62	23.40	46.05
12.00	27.81	28.32	13.06	13.45	14.01	14.82	31.71
13.00	13.10	13.51	8.00	7.75	7.66	7.96	16.10
14.00	7.63	7.77	5.81	5.40	5.28	5.30	9.30
15.00	4.85	4.96	4.62	4.15	3.97	3.91	5.96
16.00	3.50	3.53	3.80	3.42	3.21	3.13	4.13
18.00	2.17	2.18	2.91	2.56	2.40	2.30	2.44
20.00	**1.63**	**1.63**	**2.37**	**2.08**	**1.93**	**1.83**	**1.72**

Tables 2.6, 2.7, and 2.8 present the steady-state ARL values for different shifts in the Poisson mean when $\lambda_0 = 6$. These results support the conclusions found in the previous simulation results where $\lambda_0 = 10$. For small shifts in the mean, the weighted CUSUM chart slightly outperforms the standardized CUSUM chart across the values of λ, while both procedures significantly outperform the EWMA-3 procedure. We notice, for example, that when the shifted mean of interest $\lambda_1 = 7$, the weighted CUSUM and standardized CUSUM procedures have ARL values of 22.29 and 23.05 respectively at $\lambda = 7$, while the EWMA-3 chart has an ARL of 51.40.

The simulations with $\lambda_0 = 6$ also reinforce the concept of choosing the smoothing-constant value based on the size of the shift of interest. In Table 2.6, the ARL values for the EWMA-M with $r = .05$ rival the ARL values for the weighted CUSUM chart for small mean shifts. When the value of λ_1 increases from 7 to 8, as seen in Table 2.7, the best performing chart for the shift of interest is now the EWMA-M chart with $r = .1$. In Table 2.8, where $\lambda_1 = 9$, the EWMA-M chart with $r = .15$ has the quickest detection on average. Both CUSUM methods and the EWMA-M method are better at detecting small shifts in the Poisson mean compared to the EWMA-3 method. This is because the EWMA-3 chart has a smoothing constant $r = .9$, which

was recommended by Dong et al. (2008). This high value of the smoothing constant causes the statistics that are weighted by the EWMA method to be mainly based on the last two data points, much more like standard Shewhart charts. This results in a chart that detects large shifts in the mean quickly, but is less sensitive to small shifts.

Table 2.6. Comparison of ARL Values for $\lambda_0 = 6$ and $\lambda_1 = 7$ with $ARL_0 \approx 200$

λ	$h_2 = 16.14$ Weighted CUSUM	$h_1 = 5.71$ Standardized CUSUM	$L_1 = 2.24$ EWMA-M $(r = .05)$	$L_1 = 2.47$ EWMA-M $(r = .1)$	$L_1 = 2.61$ EWMA-M $(r = .15)$	$L_1 = 2.69$ EWMA-M $(r = .2)$	$L_3 = 2.89$ EWMA-3 $(r = .9)$
6.25	89.68	92.69	95.77	100.64	107.00	110.68	133.84
6.50	49.78	51.83	51.96	56.83	62.38	66.83	97.26
6.75	32.18	33.03	33.04	35.92	39.39	42.86	70.53
7.00	**22.29**	**23.05**	**22.88**	**24.41**	**26.54**	**29.12**	**51.40**
7.25	17.03	17.07	17.19	17.82	19.33	21.01	40.05
7.50	13.42	13.61	13.79	13.98	14.96	15.92	30.71
7.75	11.29	11.27	11.40	11.20	11.62	12.50	24.35
8.00	9.58	9.44	9.74	9.39	9.75	10.10	19.35
9.00	6.09	5.97	5.99	5.64	5.58	5.61	9.29
10.00	4.50	4.36	4.45	4.04	3.88	3.86	5.32
11.00	3.63	3.56	3.58	3.18	3.03	2.94	3.56
12.00	3.02	2.99	2.98	2.66	2.52	2.41	2.57
13.00	2.65	2.61	2.61	2.30	2.17	2.04	2.01
14.00	2.38	2.35	2.32	2.04	1.91	1.81	1.68

All of our simulations for constant sample sizes indicate that the weighted CUSUM chart performs well for shifts for which it is designed and also for shifts around this value. However, the EWMA-M chart has comparable performance to the weighted CUSUM charts when the appropriate smoothing constant is chosen based on the shift of interest. It is apparent that the lower smoothing constant and the lower reflecting barrier have a major impact on the performance of the EWMA chart for monitoring Poisson counts with constant sample sizes.

Table 2.7. Comparison of ARL Values for $\lambda_0 = 6$ and $\lambda_1 = 8$ with $ARL_0 \approx 200$

λ	$h_2 = 11.20$ Weighted CUSUM	$h_1 = 4.00$ Standardized CUSUM	$L_1 = 2.24$ EWMA-M $(r = .05)$	$L_1 = 2.47$ EWMA-M $(r = .1)$	$L_1 = 2.61$ EWMA-M $(r = .15)$	$L_1 = 2.69$ EWMA-M $(r = .2)$	$L_3 = 2.89$ EWMA-3 $(r = .9)$
6.25	103.50	106.15	95.77	100.64	107.00	110.68	133.84
6.50	59.54	61.62	51.96	56.83	62.38	66.83	97.26
6.75	37.54	38.93	33.04	35.92	39.39	42.86	70.53
7.00	25.50	26.76	22.88	24.41	26.54	29.12	51.40
7.25	18.46	19.40	17.19	17.82	19.33	21.01	40.05
7.50	14.53	14.92	13.79	13.98	14.96	15.92	30.71
7.75	11.40	11.62	11.40	11.20	11.62	12.50	24.35
8.00	**9.49**	**9.67**	**9.74**	**9.39**	**9.75**	**10.10**	**19.35**
9.00	5.63	5.61	5.99	5.64	5.58	5.61	9.29
10.00	4.00	3.93	4.45	4.04	3.88	3.86	5.32
11.00	3.21	3.10	3.58	3.18	3.03	2.94	3.56
12.00	2.64	2.60	2.98	2.66	2.52	2.41	2.57
13.00	2.31	2.27	2.61	2.30	2.17	2.04	2.01
14.00	2.03	1.99	2.32	2.04	1.91	1.81	1.68

Table 2.8. Comparison of ARL Values for $\lambda_0 = 6$ and $\lambda_1 = 9$ with $ARL_0 \approx 200$

λ	$h_2 = 8.61$ Weighted CUSUM	$h_1 = 3.01$ Standardized CUSUM	$L_1 = 2.24$ EWMA-M $(r = .05)$	$L_1 = 2.47$ EWMA-M $(r = .1)$	$L_1 = 2.61$ EWMA-M $(r = .15)$	$L_1 = 2.69$ EWMA-M $(r = .2)$	$L_3 = 2.89$ EWMA-3 $(r = .9)$
6.25	109.80	111.60	95.77	100.64	107.00	110.68	133.84
6.50	66.21	67.72	51.96	56.83	62.38	66.83	97.26
6.75	43.16	44.33	33.04	35.92	39.39	42.86	70.53
7.00	29.42	30.33	22.88	24.41	26.54	29.12	51.40
7.25	21.20	21.67	17.19	17.82	19.33	21.01	40.05
7.50	16.15	16.85	13.79	13.98	14.96	15.92	30.71
7.75	12.46	12.87	11.40	11.20	11.62	12.50	24.35
8.00	10.20	10.38	9.74	9.39	9.75	10.10	19.35
9.00	**5.59**	**5.63**	**5.99**	**5.64**	**5.58**	**5.61**	**9.29**
10.00	3.80	3.83	4.45	4.04	3.88	3.86	5.32
11.00	2.94	2.93	3.58	3.18	3.03	2.94	3.56
12.00	2.41	2.38	2.98	2.66	2.52	2.41	2.57
13.00	2.08	2.04	2.61	2.30	2.17	2.04	2.01
14.00	1.84	1.78	2.32	2.04	1.91	1.81	1.68

The lack of a reflecting lower barrier could also be a reason for the elevated EWMA-3 ARL values. Gan (1990) and Borror et al. (1998) used Markov chains to calculate ARL values for EWMA charts with count data and constant sample size. Gan (1990) performed ARL computations for both one-sided and two-sided charts, but Borror et al. (1998) only performed ARL computations for EWMA charts with both upper and lower control limits. We ran simulations to estimate the ARL values computed by Borror et al. (1998), but the lower bound was removed. We found that on average our ARL values for a given increase in the parameter were about 10% higher than the ARL values for the methods that have both upper and lower bounds.

Simulation Results for Varying Sample Sizes

In this section, we extend our study of the steady-state ARL performance of the proposed EWMA and CUSUM charts to varying sample size cases. By allowing the sample sizes to vary, we are able to see if the performance of the charts is consistent with our results from the fixed sample size study. Through these comparisons, we are able to recommend the methods that work best for monitoring processes with count data when the sample sizes vary randomly.

The CUSUM methods to be compared are the GLR CUSUM method based on the statistics in Equation (5), the WLR CUSUM method based on the statistics in Equation (6), and the standardized CUSUM method based on the statistics in Equation (4). One of the EWMA methods, which we will call the EWMA-1 chart, has UCLs based on the exact variances of the EWMA statistics given in Equation (8) and has $r = .9$. The second EWMA method compared is our new EWMA method, the EWMA-M chart. Like the EWMA-1 chart, the UCLs are based on the exact variance in Equation (8), but unlike the EWMA-1 chart there is a reflecting lower barrier at λ_0. We also evaluate the EWMA-M chart based on different smoothing constants, in particular for $r = .05, .1, .15, .2,$ and $.5$.

The varying sample sizes were implemented by placing a continuous uniform distribution, $U(a, b)$, $(b > a)$, on n_i for $i = 1, 2, \ldots$. Various combinations of the upper and lower limits for the uniform distribution were studied to ensure that the uniform distribution placed on the sample sizes had no influence on the relative performance of the methods. The combinations of the parameters studied were $(a, b) = (10, 15), (10, 20),$ and $(10, 50)$. The lower bound of 10 was used because this is the same minimum sample size used in Dong et al.'s

(2008) simulation study. Each of the estimated ARL values for the varying sample size cases were obtained from 10,000 simulations. The control limits were set so that the zero-state $\text{ARL}_0 = 200$. As in the constant sample size case, the process was run for 50 samples while in-control. If a simulated chart signaled during those first 50 samples, that particular run was discarded.

Because the sample sizes are varying, we are now able to distinguish between the performance of the three CUSUM methods. Table 2.9 shows estimated steady-state ARL values for all methods when $\lambda_0 = 1$ and $\lambda_1 = 1.2$ with $a = 10$ and $b = 15$. Because the sample size varies, shifts in the Poisson mean, $n_i\lambda_1, i = 1, 2, \ldots$, will also vary. The results reveal that the GLR CUSUM chart outperforms the other CUSUM methods for shifts in λ from 1 to 1.2, which corresponds to shifts in the Poisson mean as small as 10 to 12 and shifts as large as 15 to 18. The standardized CUSUM method has similar or better ARL performance beyond $\lambda = 1.2$, while both the GLR and standardized CUSUM methods have the same or better ARL performance than the WLR CUSUM methods for all shifts in the Poisson rate beyond $\lambda = 1.2$.

The CUSUM methods outperform the EWMA-1 methods except for the extremely large shifts, which is attributed to the high smoothing constant value for the EWMA-1 chart. However, the ARL performance of the EWMA-M charts is more comparable to that of the CUSUM charts. The smaller smoothing constants make the EWMA-M technique more sensitive to smaller shifts. This is shown in Table 2.9 where the EWMA-M method with $r = .05$ outperforms the CUSUM methods for shifts up to $\lambda = 1.2$. At this value the GLR CUSUM has the quickest detection, which is expected because this is the out-of-control shift for which the GLR CUSUM chart was designed to detect quickly.

The ARL comparisons for the control charting methods when $\lambda_0 = 1$ and $\lambda_1 = 1.2$ are illustrated in Figure 2.1. Each line in the graph represents the ratios of the ARL values for one of the eight control charting methods divided by the ARL values for the GLR CUSUM chart. When the ratio is greater than one, the control charting method is worse than the GLR CUSUM chart at detecting that particular shift in the Poisson rate. When the ratio is less than one, the control charting method is better than the GLR CUSUM chart at detecting that particular shift in the Poisson rate. These same ratio comparisons are given in Figures 2.2, 2.3, and 2.4 for situations where the out-of-control rate differs from 1.2.

At the shift of interest, $\lambda_1 = 1.2$, notice that the ratios for all the control charting methods are above one. This indicates the GLR CUSUM chart has the best ARL performance compared to the other control charting methods when the Poisson rate shifts to 1.2. The GLR CUSUM chart also has good ARL performance for shifts around $\lambda = 1.2$.

The ratios displayed in Figure 2.1 reinforce the recommendation that the smoothing constant for the EWMA chart should be chosen based on size of the shift one is interested in detecting. Notice that the EWMA-M chart with $r = .05$ is the best performing method for the small shifts, while the EWMA-M chart with $r = .5$ and the EWMA-1 chart with $r = .9$ perform best for large shifts in the Poisson rate.

Table 2.9. Comparison of ARL Values for $\lambda_0 = 1$ and $\lambda_1 = 1.2$, where $a = 10, b = 15$ with $ARL_0 \approx 200$.

	$h_2 = 16.97$	$h_1 = 4.37$	$h_3 = 1.38$	$L_1 = 2.24$	$L_1 = 2.45$	$L_1 = 2.57$	$L_1 = 2.65$	$L_1 = 2.84$	$L_1 = 2.82$
	GLR	Standardized	WLR	EWMA-M	EWMA-M	EWMA-M	EWMA-M	EWMA-M	EWMA-1
λ	CUSUM	CUSUM	CUSUM	$(r = .05)$	$(r = .1)$	$(r = .15)$	$(r = .2)$	$(r = .5)$	$(r = .9)$
1.025	108.71	110.59	110.01	106.52	111.11	115.56	119.59	136.01	147.38
1.05	65.24	67.04	65.82	61.16	67.44	72.22	77.60	97.67	113.75
1.075	43.13	44.65	43.72	39.77	43.02	46.70	50.89	70.07	84.84
1.1	29.27	30.04	29.57	27.77	29.63	32.83	35.82	50.51	65.68
1.15	16.92	17.23	16.94	16.67	17.13	18.20	19.92	29.42	40.98
1.2	**11.18**	**11.49**	**11.46**	**11.53**	**11.48**	**11.80**	**12.56**	**18.38**	**26.79**
1.3	6.58	6.57	6.69	7.17	6.63	6.63	6.66	8.65	13.01
1.4	4.68	4.67	4.74	5.17	4.69	4.54	4.51	5.19	7.52
1.5	3.63	3.61	3.67	4.12	3.67	3.46	3.44	3.56	4.66
1.6	2.99	3.01	3.04	3.43	3.04	2.86	2.76	2.71	3.27
1.8	2.28	2.29	2.31	2.62	2.30	2.15	2.03	1.85	1.98
2	1.89	1.90	1.90	2.15	1.88	1.74	1.66	1.44	1.45

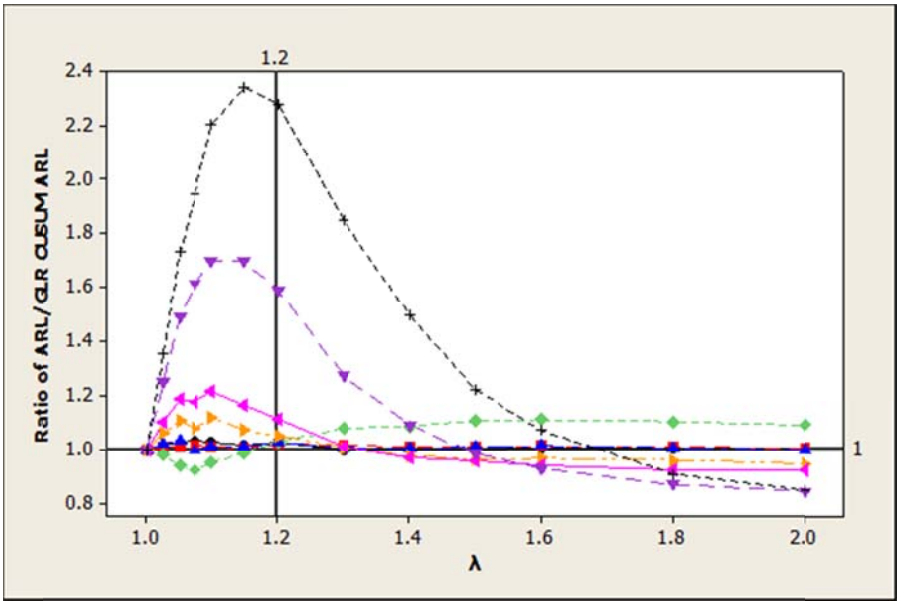

Figure 2.1 ARL Comparisons for $\lambda_0 = 1$ and $\lambda_1 = 1.2$, where $a = 10, b = 15$ with $ARL_0 \approx 200$
STD CUSUM; WLR CUSUM; EWMA-M (r =.05); EWMA-M (r =.10) EWMA-M (r =.15); EWMA-M (r =.2); EWMA-M (r =.5); EWMA-1 (r =.09)

The steady-state ARL performance for the CUSUM methods remains very similar as the value of λ_1 changes from 1.2 to 1.5. The results in Table 2.10 reveal that the GLR CUSUM technique outperforms both the standardized CUSUM method and WLR CUSUM chart at detecting increases in the Poisson rate up to the specified shift of $\lambda_1 = 1.5$. With the increase in λ_1, the EWMA-M chart with $r = .2$ has quickest detection among the other EWMA methods. This again reveals the need to choose the smoothing constant based on the size of the shift one wishes to detect. Like the previous cases, the GLR CUSUM chart has the best performance at the specified out-of-control shift $\lambda_1 = 1.5$.

Table 2.10 also shows the steady-state ARL performance for the ATM CUSUM method proposed by Mei et al. (2011), which uses the signal rule $S_{2,i} \geq n_i h_4$. They recommended the ATM CUSUM chart because the chart's performance was robust to whether the sample size was monotonically increasing or decreasing. Instead of considering monotonically increasing or decreasing sample sizes, we examined random sample sizes. The estimated ARL values in Table 2.10 indicate that the performance of the ATM CUSUM method is inferior to the performance of the other CUSUM methods and the EWMA-M and EWMA-1 methods.

Figure 2.2 illustrates graphically the comparisons displayed in Table 2.10. Similar to the conclusions gained from Figure 2.1, the GLR CUSUM chart is the best performing chart for the

shift in which the chart was designed to detect quickly, which this case is $\lambda_1 = 1.5$. This is illustrated by the fact that the ratios for all the methods are above one at $\lambda = 1.5$ indicating that the ARL_1 values for the control charting methods are all greater than the ARL_1 value for the GLR CUSUM chart. This relationship remains true for many of the shifts in the rates around $\lambda = 1.5$.

Table 2.10. Comparison of ARL Values for $\lambda_0 = 1$ and $\lambda_1 = 1.5$, where $a = 10, b = 15$ with $ARL_0 \approx 200$

λ	$h_2 = 9.04$ GLR CUSUM	$h_1 = 2.25$ Standardized CUSUM	$h_3 = .74$ WLR CUSUM	$h_4 = .58$ ATM CUSUM	$L_1 = 2.24$ EWMA-M $(r = .05)$	$L_1 = 2.45$ EWMA-M $(r = .1)$	$L_1 = 2.57$ EWMA-M $(r = .15)$	$L_1 = 2.65$ EWMA-M $(r = .2)$	$L_1 = 2.82$ EWMA-1 $(r = .9)$
1.025	130.95	131.61	131.43	154.62	106.52	115.37	115.56	119.59	147.38
1.05	90.10	91.73	91.51	119.11	61.16	69.98	72.22	77.60	113.75
1.075	63.02	63.92	63.49	91.20	39.77	44.40	46.70	50.89	84.84
1.1	45.02	46.23	45.90	72.29	27.77	30.90	32.83	35.82	65.68
1.15	24.90	25.80	25.31	46.23	16.67	17.25	18.20	19.92	40.98
1.2	15.51	16.03	15.76	30.68	11.53	11.47	11.80	12.56	26.79
1.3	7.51	7.77	7.72	15.14	7.17	6.73	6.63	6.66	13.01
1.4	4.69	4.76	4.74	8.45	5.17	4.71	4.54	4.51	7.52
1.5	**3.34**	**3.37**	**3.41**	**5.23**	**4.12**	**3.68**	**3.46**	**3.44**	**4.66**
1.6	2.65	2.65	2.66	3.58	3.43	3.05	2.86	2.76	3.27
1.8	1.87	1.86	1.90	2.09	2.62	2.32	2.15	2.03	1.98
2	1.52	1.51	1.50	1.48	2.15	1.90	1.74	1.66	1.45

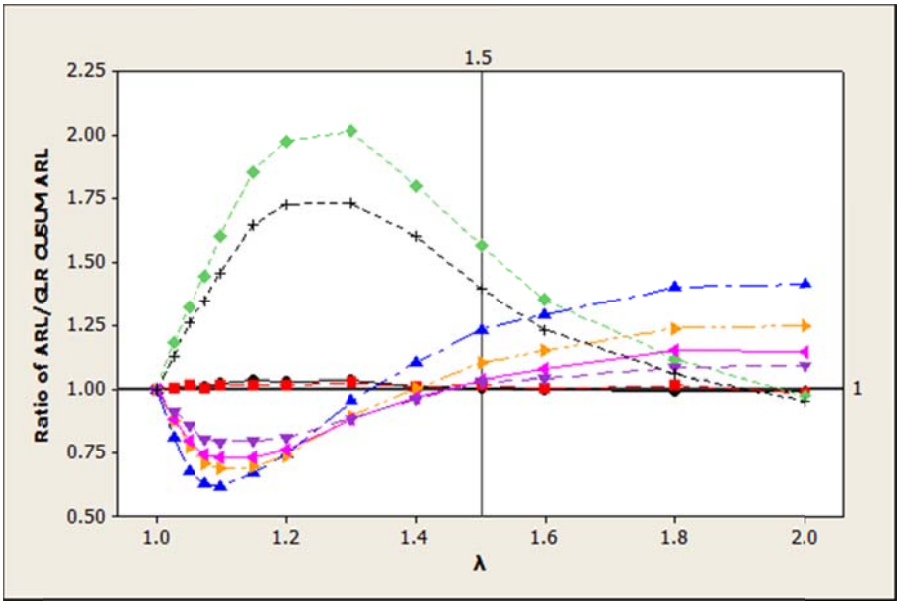

Figure 2.2 ARL Comparisons for $\lambda_0 = 1$ and $\lambda_1 = 1.5$, where $a = 10, b = 15$ with $ARL_0 \approx 200$
STD CUSUM; WLR CUSUM; ATM CUSUM; EWMA-M (r =.05)
EWMA-M (r =.1); EWMA-M (r =.15); EWMA-M (r =.2);
EWMA-1 (r =.09)

As the shift of interest increases to $\lambda_1 = 1.8$, the EWMA-M method with $r = .5$ has the best ARL performance compared to the other EWMA methods. The steady-state ARL values for the methods when $\lambda_0 = 1$ and $\lambda_1 = 1.8$ with $a = 10$ and $b = 15$ are presented in Table 2.11. As seen with the previous cases, the GLR CUSUM chart has better performance compared to other CUSUM methods for shifts up to the shift of primary interest. Notice that the EWMA-M method with $r = .05$ has much quicker performance compared to the GLR CUSUM chart for small shifts. This is due to the fact that the GLR CUSUM chart in this case is designed to detect large shifts, not small shifts. These same conclusions are illustrated in Figure 2.3.

Table 2.11. Comparison of ARL Values for $\lambda_0 = 1$ and $\lambda_1 = 1.8$ where $a = 10, b = 15$ with $ARL_0 \approx 200$

λ	$h_2 = 6.02$ GLR CUSUM	$h_1 = 1.43$ Standardized CUSUM	$h_3 = .50$ WLR CUSUM	$L_1 = 2.24$ EWMA-M $(r = .05)$	$L_1 = 2.45$ EWMA-M $(r = .1)$	$L_1 = 2.57$ EWMA-M $(r = .15)$	$L_1 = 2.65$ EWMA-M $(r = .2)$	$L_1 = 2.84$ EWMA-M $(r = .5)$	$L_1 = 2.82$ EWMA-1 $(r = .9)$
1.025	143.16	144.96	144.87	106.52	115.37	115.56	119.59	136.01	147.38
1.05	106.51	108.47	107.36	61.16	69.98	72.22	77.60	97.67	113.75
1.075	77.46	79.24	78.62	39.77	44.40	46.70	50.89	70.07	84.84
1.1	58.52	60.93	60.18	27.77	30.90	32.83	35.82	50.51	65.68
1.15	34.78	36.79	35.78	16.67	17.25	18.20	19.92	29.42	40.98
1.2	21.07	22.65	22.05	11.53	11.47	11.80	12.56	18.38	26.79
1.3	10.17	10.77	10.18	7.17	6.73	6.63	6.66	8.65	13.01
1.4	5.69	5.98	5.80	5.17	4.71	4.54	4.51	5.19	7.52
1.5	3.75	3.89	3.85	4.12	3.68	3.46	3.44	3.56	4.66
1.6	2.77	2.84	2.77	3.43	3.05	2.86	2.76	2.71	3.27
1.8	**1.83**	**1.82**	**1.85**	**2.62**	**2.32**	**2.15**	**2.03**	**1.85**	**1.98**
2	1.43	1.43	1.43	2.15	1.90	1.74	1.66	1.44	1.45

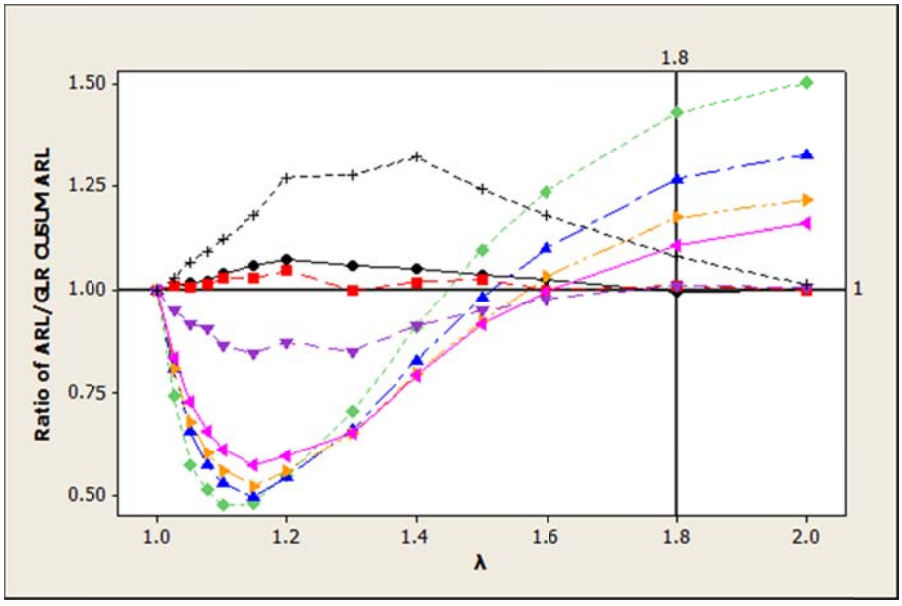

Figure 2.3. ARL Comparisons for $\lambda_0 = 1$ and $\lambda_1 = 1.8$, where $a = 10, b = 15$ with $ARL_0 \approx 200$
STD CUSUM; WLR CUSUM; EWMA-M (r =.05); EWMA-M (r =.10)
EWMA-M (r =.15); EWMA-M (r =.2); EWMA-M (r =.5);
EWMA-1 (r =.09)

Table 2.12 provides the first evidence of the EWMA-1 chart performance being comparable to that of the CUSUM methods. When the mean shift of interest has increased to a quite large value between 20 and 30, the ARL values for the EWMA-1 method and the CUSUM methods become more comparable. The EWMA-M chart with $r = .5$ and the EWMA-1 chart with $r = .9$ have similar performance at the shift of primary interest $\lambda_1 = 2$, but the GLR CUSUM chart still outperforms both EWMA methods at this shift. The improved performance for the EWMA-1 chart is also illustrated in Figure 2.4.

Table 2.12. Comparison of ARL Values for $\lambda_0 = 1$ and $\lambda_1 = 2$ where $a = 10, b = 15$ with $ARL_0 \approx 200$

	$h_2 = 4.68$	$h_1 = 1.06$	$h_3 = .39$	$L_1 = 2.24$	$L_1 = 2.45$	$L_1 = 2.57$	$L_1 = 2.65$	$L_1 = 2.84$	$L_1 = 2.82$
	GLR	Standardized	WLR	EWMA-M	EWMA-M	EWMA-M	EWMA-M	EWMA-M	EWMA-1
λ	CUSUM	CUSUM	CUSUM	$(r = .05)$	$(r = .1)$	$(r = .15)$	$(r = .2)$	$(r = .5)$	$(r = .9)$
1.025	147.06	148.81	148.44	106.52	115.37	115.56	119.59	136.01	147.38
1.05	111.54	114.58	113.44	61.16	69.98	72.22	77.60	97.67	113.75
1.075	83.41	86.41	85.36	39.77	44.40	46.70	50.89	70.07	84.84
1.1	64.44	66.83	65.58	27.77	30.90	32.83	35.82	50.51	65.68
1.15	39.43	41.54	40.92	16.67	17.25	18.20	19.92	29.42	40.98
1.2	24.88	26.69	25.79	11.53	11.47	11.80	12.56	18.38	26.79
1.3	11.69	12.57	12.05	7.17	6.73	6.63	6.66	8.65	13.01
1.4	6.52	7.07	6.91	5.17	4.71	4.54	4.51	5.19	7.52
1.5	4.13	4.39	4.28	4.12	3.68	3.46	3.44	3.56	4.66
1.6	2.97	3.08	2.99	3.43	3.05	2.86	2.76	2.71	3.27
1.8	1.87	1.91	1.89	2.62	2.32	2.15	2.03	1.85	1.98
2	**1.41**	**1.43**	**1.43**	**2.15**	**1.90**	**1.74**	**1.66**	**1.44**	**1.45**

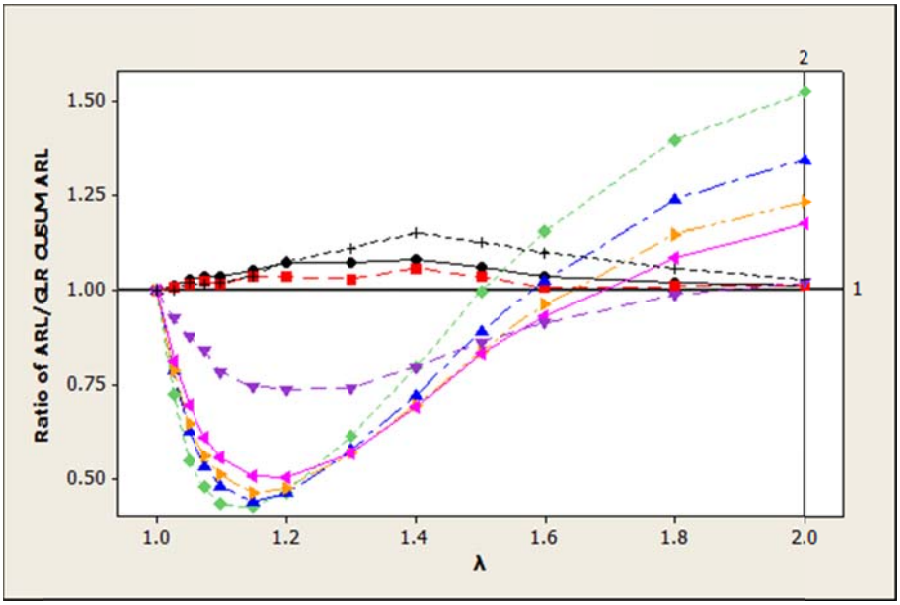

Figure 2.4. ARL Comparisons for $\lambda_0 = 1$ and $\lambda_1 = 2$, where $a = 10, b = 15$ with $ARL_0 \approx 200$
STD CUSUM; WLR CUSUM; EWMA-M (r =.05); EWMA-M (r =.10) EWMA-M (r =.15); EWMA-M (r =.2); EWMA-M (r =.5); EWMA-1 (r =.09)

Simulations were also conducted where the sample sizes were drawn from uniform distributions with different parameters. The $U(10, 20)$and $U(10, 50)$ cases were explored to determine if changing the parameters of the uniform distribution had any influence on the relative ARL performance of the control chart methods in this paper. The results follow closely to the cases previously discussed where the $U(10, 15)$ distribution was used to draw samples sizes. However, when the value of b was increased to 20 and 50 and the shift of interest was large, the performance of the EWMA-1 method compared to the other control chart methods was even better than the performance of the EWMA-1 method displayed in Table 2.12 when $b = 15$. The improved performance of the EWMA-1 method is shown in Table 2.13. The reason the EWMA-1 method performs better is because the shift in the means of the Poisson random variables increases as the sample sizes increase. All ARL comparisons for $U(10, 20)$ and the remaining ARL comparisons for $U(10, 50)$ are given the appendix.

Table 2.13. Comparison of ARL Values for $\lambda_0 = 1$ and $\lambda_1 = 2$ where $a = 10, b = 50$ with $\text{ARL}_0 \approx 200$

λ	$h_2 = 2.82$ GLR CUSUM	$h_3 = .16$ WLR CUSUM	$h_1 = .46$ Standardized CUSUM	$L_1 = 2.21$ EWMA-M $(r = .05)$	$L_1 = 2.43$ EWMA-M $(r = .1)$	$L_1 = 2.54$ EWMA-M $(r = .15)$	$L_1 = 2.61$ EWMA-M $(r = .2)$	$L_1 = 2.77$ EWMA-M $(r = .5)$	$L_1 = 2.75$ EWMA-1 $(r = .9)$
1.025	145.13	152.00	149.96	83.06	89.53	95.57	99.11	115.05	130.39
1.05	106.33	117.65	113.26	42.12	45.41	50.28	53.55	71.40	86.34
1.075	77.37	89.52	84.92	25.11	26.93	29.63	31.81	44.50	58.15
1.1	56.69	69.70	64.90	17.47	18.26	19.09	20.85	29.38	40.34
1.15	31.45	40.55	37.49	10.49	10.13	10.33	10.65	14.44	21.27
1.2	18.60	25.29	23.07	7.41	6.94	6.90	6.89	8.40	12.31
1.3	7.60	10.39	9.52	4.76	4.26	3.99	3.90	4.03	5.22
1.4	3.84	4.91	4.61	3.54	3.13	2.89	2.79	2.59	2.93
1.5	2.33	2.85	2.71	2.86	2.52	2.33	2.21	1.96	2.01
1.6	1.68	1.94	1.82	2.43	2.13	1.96	1.86	1.59	1.57
1.8	1.20	1.27	1.24	1.92	1.68	1.53	1.44	1.23	1.20
2	**1.06**	**1.08**	**1.07**	**1.62**	**1.40**	**1.26**	**1.20**	**1.10**	**1.08**

Simulation Results for a Poisson Process with Low Counts

The in-control mean in the previous simulation study is at least ten. In this section we extend our study of control charts for varying sample sizes to situations where the in-control mean is small. In practice, processes with small Poisson rates are referred to as low-defect-rate processes. Saniga et al. (2009) presented a case study exploring count data where the counts were low. They modeled these counts using the binomial distribution; however, their methods could be adapted to handle Poisson count data. Saniga et al. (2009) focused on Phase I methods and concluded that that the best procedure for evaluating the capability and performance of a process was to use CUSUM and Shewhart charts simultaneously. Unlike Saniga et al. (2009) we focus on Phase II performance analyses. This section is composed of steady-state ARL comparisons for EWMA charts and CUSUM charts when the minimum in-control mean is one.

Each of the estimated steady-state ARL values for the varying sample size cases were obtained from 100,000 simulations. The control limits were set so that the zero-state $\text{ARL}_0 = 200$. As in previous simulations, the process was run for 50 samples while in-control. If a simulated chart signaled during those first 50 samples, that particular run was discarded. The

varying sample size was implemented by placing a continuous uniform distribution, $U(10, 15)$, on n_i for $i = 1, 2, \ldots$. The in-control Poisson rate for all simulations is $\lambda_0 = .1$.

The ARL performance for the GLR CUSUM chart, standardized CUSUM chart, WLR CUSUM chart, EWMA charts with $r = .05, .1, .15, .2, .5$ and a reflecting lower barrier at $\lambda_0 = .1$, and an EWMA chart with $r = .9$ and no reflecting lower barrier is compared. However, the form of the GLR CUSUM chart slightly differs from Equation (5). Rather than dividing out the constant $\ln\left\{\frac{\lambda_1}{\lambda_0}\right\}$ during the derivation of the CUSUM statistic, we leave this constant in our GLR CUSUM chart formulation. This leads to less variability in h_2, the decision interval for the GLR CUSUM chart. The value of h_2 in the simulation study with λ_0=10 ranges from 16.97 to 4.68, as displayed in Tables 2.9 through 2.12. The range of h_2 is much smaller for the current simulation study, 3.56 to 2.82, because $\ln\left\{\frac{\lambda_1}{\lambda_0}\right\}$ remains as part of the GLR CUSUM statistics. The revised GLR CUSUM statistics are

$$S_{2,i} = \max\left(0, S_{2,i-1} + \ln\left\{\frac{\lambda_1}{\lambda_0}\right\}\left[X_i - \frac{n_i(\lambda_1 - \lambda_0)}{\ln\{\lambda_1\} - \ln\{\lambda_0\}}\right]\right), i = 1, 2, \ldots, \qquad (11)$$

where $S_{2,0} = 0$. The chart signals if $S_{2,i} \geq h_2$.

The ARL performance for all control charting methods for a Poisson process with an in-control rate of $\lambda_0 = .1$ and an out-of-control rate of $\lambda_1 = .2$ is given in Table 2.14. Recall that the varying sample sizes lead to an in-control Poisson mean as small as 1 and an out-of-control Poisson mean as large as 3. The results are very similar to those given for Poisson processes with larger means. The GLR CUSUM chart is performing best for the out-of-control shift in which the chart was designed to detect, $\lambda_1 = .2$. The performance for the EWMA charts support the suggestion that the smoothing constant should be chosen based on the shift of interest. Notice that for small shifts the EWMA-M chart with $r = .05$ has the quickest detection, while the EWMA-M chart with $r = .5$ has the best detection for large shifts. The EWMA-1 chart with a smoothing constant of .9 begins to have better performance for the larger shifts, but again this chart is at a disadvantage because there is no reflecting lower barrier in place.

Table 2.14. Comparison of ARL Values for $\lambda_0 = .1$ and $\lambda_1 = .2$ where $a = 10, b = 15$ with $ARL_0 \approx 200$

λ	$h_2 = 2.82$ GLR CUSUM	$h_3 = .16$ WLR CUSUM	$h_1 = .46$ Standardized CUSUM	$L_1 = 2.33$ EWMA-M ($r = .05$)	$L_1 = 2.61$ EWMA-M ($r = .1$)	$L_1 = 2.77$ EWMA-M ($r = .15$)	$L_1 = 2.89$ EWMA-M ($r = .2$)	$L_1 = 3.25$ EWMA-M ($r = .5$)	$L_1 = 3.28$ EWMA-1 ($r = .9$)
0.11	101.55	102.24	106.36	92.69	97.60	102.41	105.49	123.15	130.78
0.12	58.17	58.65	62.23	49.45	53.90	58.09	61.73	78.77	90.21
0.13	36.78	37.20	39.82	30.86	33.51	36.46	39.03	53.45	64.32
0.14	25.20	25.44	27.39	21.67	23.12	24.87	26.67	37.79	47.56
0.15	18.29	18.52	19.76	16.44	17.10	18.14	19.51	27.81	35.94
0.16	14.02	14.22	15.06	13.14	13.28	14.02	14.83	21.06	27.95
0.17	11.24	11.38	11.96	10.92	10.88	11.23	11.79	16.45	22.18
0.18	9.34	9.42	9.84	9.35	9.21	9.34	9.69	13.27	18.06
0.20	**6.89**	**6.99**	**7.12**	**7.26**	**6.94**	**6.94**	**7.08**	**9.10**	**12.40**
0.22	5.45	5.52	5.57	5.97	5.60	5.53	5.54	6.72	9.08
0.24	4.50	4.56	4.55	5.09	4.71	4.57	4.57	5.26	6.85
0.30	3.05	3.07	3.04	3.55	3.22	3.08	3.00	3.11	3.73
0.40	2.05	2.07	2.05	2.46	2.21	2.09	2.01	1.90	2.02
0.50	1.61	1.61	1.62	2.13	1.73	1.64	1.57	1.44	1.46

As λ_1 increases, the best value for the smoothing constant of the EWMA chart also increases. The ARL results for a Poisson process with $\lambda_0 = .1$ and $\lambda_1 = .3$ and a Poisson process with $\lambda_0 = .1$ and $\lambda_1 = .4$ are given in Tables 2.15 and 2.16. When $\lambda_1 = .3$, the best preforming EWMA chart at that shift of interest is the EWMA-M chart with $r = .2$. When λ_1 increases to .4, the best performing EWMA chart at that particular shift is the chart with $r = .5$. However, the overall best performing chart at the shift of interest in both cases is the GLR CUSUM chart.

Table 2.15. Comparison of ARL Values for $\lambda_0 = .1$ and $\lambda_1 = .3$ where $a = 10, b = 15$ with $ARL_0 \approx 200$

λ	$h_2 = 3.56$ GLR CUSUM	$h_3 = .265$ WLR CUSUM	$h_1 = 2.11$ Standardized CUSUM	$L_1 = 2.33$ EWMA-M $(r = .05)$	$L_1 = 2.61$ EWMA-M $(r = .1)$	$L_1 = 2.77$ EWMA-M $(r = .15)$	$L_1 = 2.89$ EWMA-M $(r = .2)$	$L_1 = 3.25$ EWMA-M $(r = .5)$	$L_1 = 3.28$ EWMA-1 $(r = .9)$
0.11	116.29	118.32	119.99	92.69	97.60	102.41	105.49	123.15	130.78
0.12	72.26	73.23	75.87	49.45	53.90	58.09	61.73	78.77	90.21
0.13	47.74	48.87	51.15	30.86	33.51	36.46	39.03	53.45	64.32
0.14	33.16	33.93	36.02	21.67	23.12	24.87	26.67	37.79	47.56
0.15	24.16	24.72	26.36	16.44	17.10	18.14	19.51	27.81	35.94
0.16	18.17	18.62	19.76	13.14	13.28	14.02	14.83	21.06	27.95
0.17	14.17	14.53	15.53	10.92	10.88	11.23	11.79	16.45	22.18
0.18	11.49	11.72	12.48	9.35	9.21	9.34	9.69	13.27	18.06
0.20	7.98	8.14	8.60	7.26	6.94	6.94	7.08	9.10	12.40
0.22	5.99	6.13	6.35	5.97	5.60	5.53	5.54	6.72	9.08
0.24	4.77	4.87	5.00	5.09	4.71	4.57	4.57	5.26	6.85
0.30	**2.97**	**3.00**	**3.02**	**3.55**	**3.22**	**3.08**	**3.00**	**3.11**	**3.73**
0.40	1.89	1.92	1.89	2.46	2.21	2.09	2.01	1.90	2.02
0.50	1.47	1.48	1.45	2.13	1.73	1.64	1.57	1.44	1.46

Table 2.16. Comparison of ARL Values for $\lambda_0 = .1$ and $\lambda_1 = .4$ where $a = 10, b = 15$ with $ARL_0 \approx 200$

λ	$h_2 = 3.43$ GLR CUSUM	$h_3 = .201$ WLR CUSUM	$h_1 = 1.465$ Standardized CUSUM	$L_1 = 2.33$ EWMA-M $(r = .05)$	$L_1 = 2.61$ EWMA-M $(r = .1)$	$L_1 = 2.77$ EWMA-M $(r = .15)$	$L_1 = 2.89$ EWMA-M $(r = .2)$	$L_1 = 3.25$ EWMA-M $(r = .5)$	$L_1 = 3.28$ EWMA-1 $(r = .9)$
0.11	125.02	125.46	128.06	92.69	97.60	102.41	105.49	123.15	130.78
0.12	81.40	81.78	85.17	49.45	53.90	58.09	61.73	78.77	90.21
0.13	56.15	56.50	60.02	30.86	33.51	36.46	39.03	53.45	64.32
0.14	39.82	40.19	43.07	21.67	23.12	24.87	26.67	37.79	47.56
0.15	29.56	29.98	32.40	16.44	17.10	18.14	19.51	27.81	35.94
0.16	22.13	22.36	24.52	13.14	13.28	14.02	14.83	21.06	27.95
0.17	17.32	17.65	19.29	10.92	10.88	11.23	11.79	16.45	22.18
0.18	14.06	14.22	15.59	9.35	9.21	9.34	9.69	13.27	18.06
0.20	9.48	9.58	10.50	7.26	6.94	6.94	7.08	9.10	12.40
0.22	6.97	7.08	7.66	5.97	5.60	5.53	5.54	6.72	9.08
0.24	5.38	5.45	5.87	5.09	4.71	4.57	4.57	5.26	6.85
0.30	3.12	3.15	3.29	3.55	3.22	3.08	3.00	3.11	3.73
0.40	**1.89**	**1.90**	**1.91**	**2.46**	**2.21**	**2.09**	**2.01**	**1.90**	**2.02**
0.50	1.43	1.44	1.42	2.13	1.73	1.64	1.57	1.44	1.46

Table 2.17 displays the ARL values for a Poisson process with an in-control mean as small as one and an out-of-control mean as large as 7.5. These are the largest shifts studied for the low-count Poisson processes. At the shift of interest ($\lambda_1 = .5$), the performance of the CUSUM methods and the EWMA-M chart with $r = .5$ is similar.

Table 2.17. Comparison of ARL Values for $\lambda_0 = .1$ and $\lambda_1 = .5$ where $a = 10, b = 15$ with $ARL_0 \approx 200$

	$h_2 = 3.11$	$h_3 = .156$	$h_1 = .96$	$L_1 = 2.33$	$L_1 = 2.61$	$L_1 = 2.77$	$L_1 = 2.89$	$L_1 = 3.25$	$L_1 = 3.28$
	GLR	WLR	Standardized	EWMA-M	EWMA-M	EWMA-M	EWMA-M	EWMA-M	EWMA-1
λ	CUSUM	CUSUM	CUSUM	($r = .05$)	($r = .1$)	($r = .15$)	($r = .2$)	($r = .5$)	($r = .9$)
0.11	129.08	129.50	132.33	92.69	97.60	102.41	105.49	123.15	130.78
0.12	86.30	86.75	89.94	49.45	53.90	58.09	61.73	78.77	90.21
0.13	61.26	61.32	65.27	30.86	33.51	36.46	39.03	53.45	64.32
0.14	44.14	44.33	47.62	21.67	23.12	24.87	26.67	37.79	47.56
0.15	33.21	33.38	36.01	16.44	17.10	18.14	19.51	27.81	35.94
0.16	25.22	25.28	27.80	13.14	13.28	14.02	14.83	21.06	27.95
0.17	19.89	20.00	22.05	10.92	10.88	11.23	11.79	16.45	22.18
0.18	16.05	16.13	17.80	9.35	9.21	9.34	9.69	13.27	18.06
0.20	10.83	10.89	12.14	7.26	6.94	6.94	7.08	9.10	12.40
0.22	7.88	7.92	8.85	5.97	5.60	5.53	5.54	6.72	9.08
0.24	6.05	6.06	6.68	5.09	4.71	4.57	4.57	5.26	6.85
0.30	3.34	3.36	3.59	3.55	3.22	3.08	3.00	3.11	3.73
0.40	1.92	1.92	1.98	2.46	2.21	2.09	2.01	1.90	2.02
0.50	**1.43**	**1.43**	**1.45**	**2.13**	**1.73**	**1.64**	**1.57**	**1.44**	**1.46**

The ARL performance for Poisson processes with low counts and varying sample sizes closely resembles the ARL performance for Poisson processes with higher counts and varying sample sizes and Poisson processes with a fixed sample size. The GLR CUSUM chart continues to have quick detection at the out-of-control shift for which the chart is designed to detect quickly. Also, the EWMA-M chart has comparable ARL performance when the smoothing constant is selected based on the size of the out-of-control shift one is interested in detecting. The performance of the EWMA-1 chart is only comparable for large shifts like those shifts given in Table 2.17. Also, the alternative formulation for the GLR CUSUM chart given in Equation (11) does not affect the ARL performance for the chart and the decision intervals are less variable,

which could lessen simulation time when determining the values of h_2 for specified in-control ARL values.

Example

To illustrate the use of the EWMA charts and CUSUM charts, we reexamined the example provided by Dong et al. (2008). The dataset in Table 2.18 displays counts of adverse events for a product in a pharmaceutical company. We let X_i stand for the adverse event count, while n_i is the product exposure in (millons) for each quarter between July 1, 1999 and December 31, 2004, for $i = 1, 2, \dots, 22$. We consider the GLR CUSUM chart, the EWMA-1 chart with the UCLs in Equation (8), the Phase II u-chart with the control limits given in Equation (2), and the EWMA-M chart based on the exact variances in Equation (8) with $r = .2$ and a reflecting barrier at $\lambda_0 = 4$. We used $r = .9$ for the smoothing constant associated with the EWMA-1 chart, which is the same value used by Dong et al. (2008). We also considered the in-control incidence rate of $\lambda_0 = 4$ and the out-of-control incidence rate of $\lambda_1 = 7$, as did Dong et al. (2008).

We treated the data in Table 2.18 as Phase II data. The values of L_1 for the EWMA-1 chart and EWMA-M chart, L_u for the u-chart, and h_2 for the GLR CUSUM chart were found through a simulation study with 10,000 replications, where the ARL_0 value was set to 100. The varying sample sizes used for the simulations were sampled with replacement from the product exposures given in Table 2.18. The simulation led to the constants $L_1 = 2.697$ for the EWMA-1 chart, $L_1 = 2.43$ for the EWMA-M chart, $L_u = 2.687$ for the Phase II u-chart, and $h_2 = 4.96$ for the GLR CUSUM chart. Note that the value L_1 for the EWMA-1 used by Dong et al. (2008) to obtain $\text{ARL}_0 \geq 100$ was $L_1 = 2.3263$. This value was found using approximate analytical bounds derived by Dong et al. (2008). Our simulation study yielded a more accurate value of L_1, which we used to construct our EWMA-1 control chart.

Table 2.18. The Number of Adverse Events, Product Exposures and Rate for Each Quarter Reported During July 1, 1999-December 31, 2004

Time i	Adverse Event Count X_i	Product Exposure n_i (in millions)	Rate (Per Million Units)
1	1	0.206	4.854
2	0	0.313	0.000
3	0	0.368	0.000
4	0	0.678	0.000
5	1	0.974	1.027
6	0	0.927	0.000
7	3	0.814	3.686
8	3	0.696	4.310
9	3	0.659	4.552
10	2	0.775	2.581
11	5	0.731	6.840
12	5	0.71	7.042
13	2	0.705	2.837
14	4	0.754	5.305
15	4	0.682	5.865
16	3	0.686	4.373
17	4	0.763	5.242
18	3	0.833	3.601
19	8	0.738	10.840
20	3	0.741	4.049
21	2	0.843	2.372
22	2	0.792	2.525

Figures 2.5, 2.6, 2.7, and 2.8 depict the plots of the GLR CUSUM chart, the *u*-chart, the EWMA-1 chart, and the EWMA-M chart, respectively. The *u*-chart, the EWMA-1 chart, and the EWMA-M chart alarm at time point 19, which is in the first quarter of 2004. The signaling of the Shewhart *u*-chart at time point 19 is expected because there is a sharp spike in the incidence rate. Likewise, we also expect the EWMA-1 chart to signal at time point 19 because the large smoothing constant $r = .9$ causes the EWMA-1 chart to behave similarly to the Shewhart *u*-chart. The EWMA-M chart with the reflecting barrier also signals at time point 19. Even though the EWMA-M chart has a smaller smoothing constant compared to the EWMA-1 chart, the

EWMA-M chart is still able to detect the spike in the incidence rate. On the contrary, the CUSUM chart fails to alarm at time point 19 because it is less sensitive to a single large observed count. This example illustrates the similarities between the EWMA-1 chart with $r = .9$ and the Shewhart *u*-chart and also shows that a EWMA chart with a smaller smoothing constant can detect large spikes in the incidence rate.

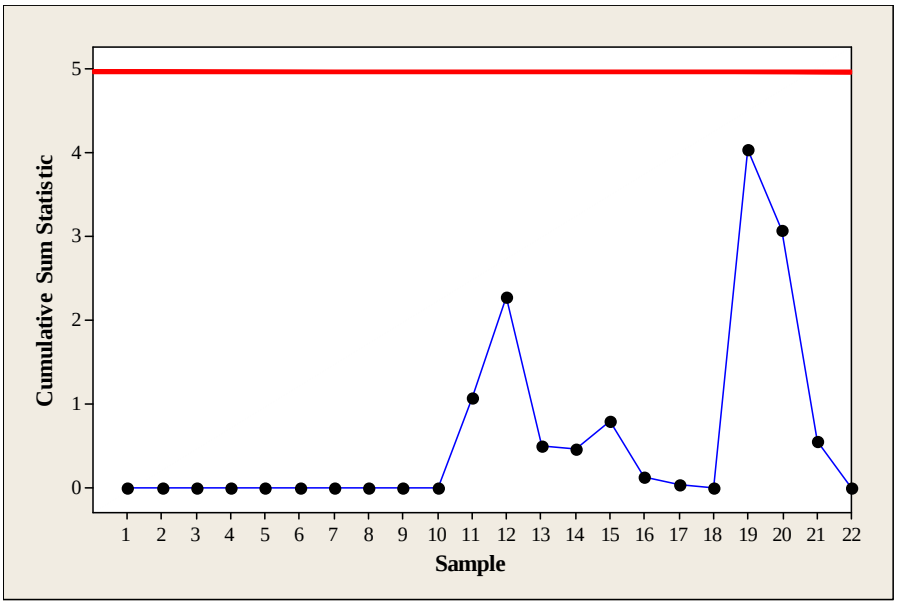

Figure 2.5. GLR CUSUM Chart, where $\lambda_0 = 4$ for the Drug-Adverse Event Example.

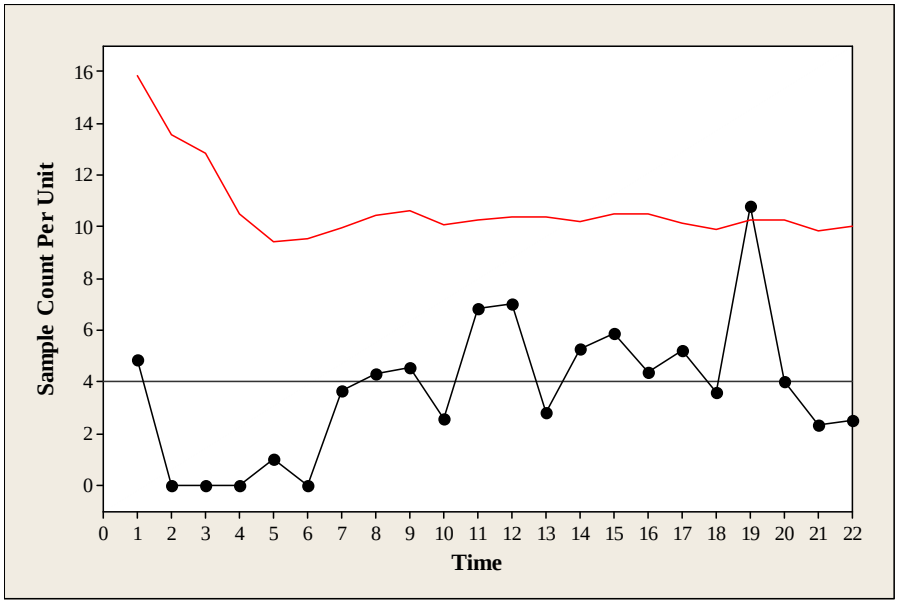

Figure 2.6. *u*-Chart, where $\lambda_0 = 4$ for the Drug-Adverse Event Example.

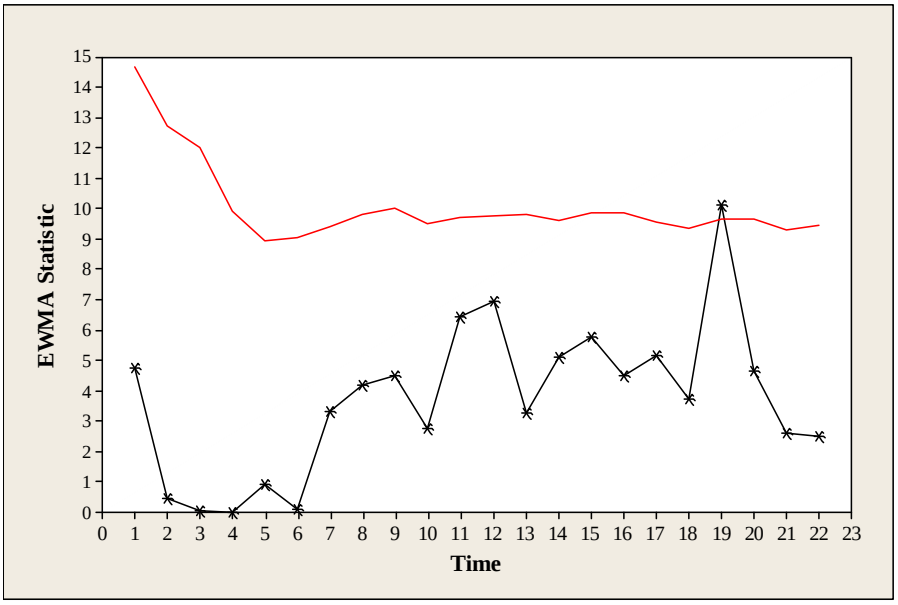

Figure 2.7. EWMA-1 Chart, where $\lambda_0 = 4$ for the Drug-Adverse Event Example.

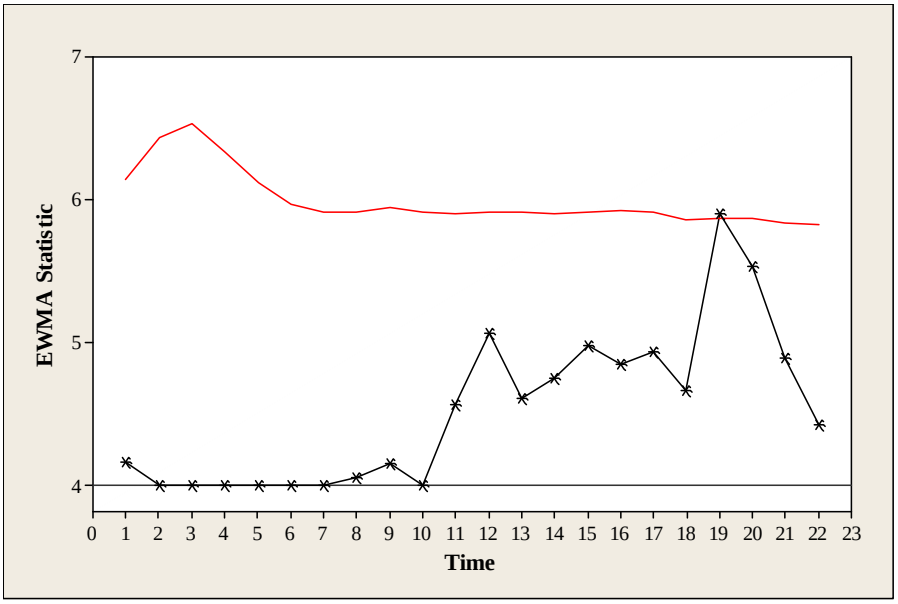

Figure 2.8. EWMA-M Chart, where $\lambda_0 = 4$ for the Drug-Adverse Event Example.

Conclusions

The results from our simulation study reveal that the GLR CUSUM chart has superior ARL performance at the out-of-control shift for which the chart is designed to detect quickly compared with the standardized CUSUM chart and WLR CUSUM chart. The GLR CUSUM chart also has quick detection at ranges of shifts around this specified shift.

The newly introduced EWMA-M charts have good ARL properties at detecting various parameter shifts. The features of the EWMA-M chart include using control limits based on the exact variances of the EWMA statistics, so there is no issue of an unknown minimum sample size in Phase II, implementing a reflecting lower barrier to protect against inertial problems, and choosing the smoothing constant for the chart based on the primary shift of interest. Through our simulation study for varying samples sizes, we see that the GLR CUSUM chart always has smaller steady-state ARL values at the out-of-control shift for which it was designed to detect, but an EWMA-M chart with the appropriate smoothing constant has comparable ARL performance at the out-of-control shift of interest and in some cases has better ARL performance for ranges of shifts around the specified out-of-control shift. One minor drawback to the EWMA-M chart is having to determine the value of the smoothing constant, r.

The results from our simulations both with fixed sample sizes and varying sample sizes indicate that the CUSUM methods and the EWMA-M methods outperform the EWMA methods of Dong et al. (2008) in detecting small shifts in the Poisson rates. We were not surprised that the EWMA methods recommended by Dong et al. (2008) did a good job detecting large shifts in the rates because they used $r = .9$. These EWMA charts were much like Shewhart charts, which are known to be able to quickly detect large shifts in the parameter of interest.

It is assumed that the observed counts in our paper are independent Poisson observations where the both the in-control mean and out-of-control mean are specified. A more general approach is to instead estimate the in-control mean at each time point. The out-of-control mean could then be computed based on the increase or decrease in the in-control mean one wishes to detect. Höhle and Paul (2008) studied the performance for different control charts in situations where the in-control mean was estimated at each time point using a seasonal log-linear model. The out-of-control mean was then characterized by a multiplicative shift.

Höhle and Paul (2008) compared the ARL performance for the following four control charts: a CUSUM chart based on the likelihood-ratio formulation (equivalent to our GLR CUSUM chart), Rossi et al.'s (1999) standardized CUSUM chart with the fixed reference limit, Rogerson and Yamada's (2004) time-varying Poisson CUSUM chart, and the generalized likelihood-ratio chart (GLR chart). Rogerson and Yamada's (2004) time-varying Poisson CUSUM chart follows closely to the CUSUM chart based on the likelihood-ratio formulation; however, they incorporated a scaling factor to determine the contribution of the observed counts

to the cumulative sum. The scaling factor is a ratio of the overall decision interval and the time varying decision intervals, where the overall decision interval is determined using the Poisson CUSUM chart with a constant mean based on the mean of the time varying parameter and the specified ARL_0. The time-varying decision intervals are determined using the varying means at each time point and the specified ARL_0. The GLR chart involves the maximization of the log-likelihood ratio across all possible shifts.

The simulation study performed by Höhle and Paul (2008) revealed that the CUSUM chart based on the likelihood-ratio formulation performed well for the shift in which the chart was designed to detect and also for shifts close to the shift of interest. The GLR control chart performed well for many of the smaller shifts, while the standardized CUSUM chart did not perform well at even meeting the specified in-control ARL. Rogerson and Yamada's (2004) time-varying Poisson CUSUM chart had comparable performance with the GLR chart and the likelihood-ratio CUSUM chart, but the time-varying Poisson CUSUM chart was never the best performing chart.

Using techniques like Poisson regression allows for more flexibility when estimating the in-control means. Höhle and Paul (2008) provided a detailed analysis regarding the performance for CUSUM procedures and the GLR chart. In future research, it would be of interest to compare the performance of these charts with the EWMA chart where the smoothing constant is chosen based on the size of the shift one is interested in detecting.

Also, in future research, it would be important to study the effects of estimation error on the performance of the CUSUM charts and EWMA charts compared in our paper. The EWMA and CUSUM charts are designed assuming that the in-control Poisson rate, λ_0, is estimated without error during a Phase I analysis or as in Höhle and Paul's (2008) research using Poisson regression. However, in practice we know estimation error does exist. Jensen et al. (2006) gave a literature review on the effects of parameter estimation on control chart properties.

The control charts in our paper are based on Poisson count data that are assumed to be independent observations. However, in practice there may be situations where autocorrelation in the samples exists. A future research topic could be studying the effect of autocorrelation on the performance of the charts discussed in our paper. Weiss and Testik (2009) studied a CUSUM chart based on a Poisson integer-valued autoregressive model of order 1, where the sample size remains constant. This CUSUM chart monitors both the Poisson mean and changes in the

autocorrelation structure. It would be of interest to extend this CUSUM chart that monitors both the Poisson mean and the autocorrelation structure to situations where the sample sizes vary.

Appendix A: ARL Comparisons for $U(10, 20)$ and $U(10, 50)$

Table 2.A1. Comparison of ARL Values for $\lambda_0 = 1$ and $\lambda_1 = 1.2$ where $a = 10, b = 20$ with $ARL_0 \approx 200$

λ	$h_2 = 17.491$ GLR CUSUM	$h_1 = 4.145$ Standardized CUSUM	$h_3 = 1.21$ WLR CUSUM	$L_1 = 2.24$ EWMA-M $(r = .05)$	$L_1 = 2.45$ EWMA-M $(r = .1)$	$L_1 = 2.57$ EWMA-M $(r = .15)$	$L_1 = 2.64$ EWMA-M $(r = .2)$	$L_1 = 2.83$ EWMA-M $(r = .5)$	$L_1 = 2.80$ EWMA-1 $(r = .9)$
1.025	105.12	106.86	106.92	109.11	112.71	116.45	134.36	142.26	142.26
1.05	62.23	63.27	63.02	63.81	69.80	72.52	91.29	106.57	106.57
1.075	40.64	41.24	40.89	40.37	44.59	47.62	66.17	78.79	78.79
1.1	26.99	28.25	28.25	28.53	31.14	32.81	47.00	59.78	59.78
1.15	15.01	15.34	15.49	16.53	17.44	18.17	26.92	36.39	36.39
1.2	**10.06**	**10.09**	**10.15**	**11.19**	**11.40**	**11.62**	**16.29**	**23.44**	**23.44**
1.3	5.77	5.82	5.94	6.87	6.59	6.55	7.64	10.93	10.93
1.4	4.12	4.16	4.21	4.99	4.64	4.48	4.67	6.04	6.04
1.5	3.24	3.25	3.30	3.97	3.68	3.47	3.26	3.82	3.82
1.6	2.71	2.71	2.74	3.31	3.02	2.86	2.56	2.71	2.71
1.8	2.06	2.07	2.07	2.55	2.31	2.15	1.80	1.71	1.71
2	1.69	1.72	1.72	2.11	1.90	1.78	1.42	1.31	1.31

Table 2.A2. Comparison of ARL Values for $\lambda_0 = 1$ and $\lambda_1 = 1.5$ where $a = 10, b = 20$ with $ARL_0 \approx 200$

λ	$h_2 = 9.04$ GLR CUSUM	$h_1 = 2.0815$ Standardized CUSUM	$h_3 = .641$ WLR CUSUM	$L_1 = 2.24$ EWMA-M $(r = .05)$	$L_1 = 2.45$ EWMA-M $(r = .1)$	$L_1 = 2.57$ EWMA-M $(r = .15)$	$L_1 = 2.64$ EWMA-M $(r = .2)$	$L_1 = 2.83$ EWMA-M $(r = .5)$	$L_1 = 2.80$ EWMA-1 $(r = .9)$
1.025	128.95	130.53	132.54	104.53	109.11	112.71	116.45	134.36	142.26
1.05	87.94	89.64	91.41	60.63	63.81	69.80	72.52	91.29	106.57
1.075	59.71	62.06	63.34	38.11	40.37	44.59	47.62	66.17	78.79
1.1	42.39	44.51	45.36	27.36	28.53	31.14	32.81	47.00	59.78
1.15	23.25	24.59	24.56	16.72	16.53	17.44	18.17	26.92	36.39
1.2	13.83	14.53	14.72	11.97	11.19	11.40	11.62	16.29	23.44
1.3	6.61	6.90	7.01	7.65	6.87	6.59	6.55	7.64	10.93
1.4	4.10	4.22	4.28	5.75	4.99	4.64	4.48	4.67	6.04
1.5	**2.95**	**2.96**	**3.07**	**4.62**	**3.97**	**3.68**	**3.47**	**3.26**	**3.82**
1.6	2.34	2.34	2.43	3.90	3.31	3.02	2.86	2.56	2.71
1.8	1.68	1.66	1.73	3.06	2.55	2.31	2.15	1.80	1.71
2	1.36	1.35	1.38	2.54	2.11	1.90	1.78	1.42	1.31

Table 2.A3. Comparison of ARL Values for $\lambda_0 = 1$ and $\lambda_1 = 1.8$ where $a = 10, b = 20$ with $ARL_0 \approx 200$

λ	$h_2 = 5.836$ GLR CUSUM	$h_1 = 1.29$ Standardized CUSUM	$h_3 = .4229$ WLR CUSUM	$L_1 = 2.24$ EWMA-M $(r = .05)$	$L_1 = 2.45$ EWMA-M $(r = .1)$	$L_1 = 2.57$ EWMA-M $(r = .15)$	$L_1 = 2.64$ EWMA-M $(r = .2)$	$L_1 = 2.83$ EWMA-M $(r = .5)$	$L_1 = 2.80$ EWMA-1 $(r = .9)$
1.025	140.84	143.93	144.94	104.53	109.11	112.71	116.45	134.36	142.26
1.05	104.03	108.45	109.17	60.63	63.81	69.80	72.52	91.29	106.57
1.075	74.02	77.60	78.51	38.11	40.37	44.59	47.62	66.17	78.79
1.1	55.41	59.06	59.17	27.36	28.53	31.14	32.81	47.00	59.78
1.15	31.85	34.66	34.87	16.72	16.53	17.44	18.17	26.92	36.39
1.2	19.52	21.49	21.27	11.97	11.19	11.40	11.62	16.29	23.44
1.3	8.86	9.69	9.54	7.65	6.87	6.59	6.55	7.64	10.93
1.4	4.96	5.31	5.21	5.75	4.99	4.64	4.48	4.67	6.04
1.5	3.29	3.46	3.44	4.62	3.97	3.68	3.47	3.26	3.82
1.6	2.44	2.51	2.53	3.90	3.31	3.02	2.86	2.56	2.71
1.8	**1.65**	**1.66**	**1.68**	**3.06**	**2.55**	**2.31**	**2.15**	**1.80**	**1.71**
2	1.29	1.30	1.32	2.54	2.11	1.90	1.78	1.42	1.31

Table 2.A4. Comparison of ARL Values for $\lambda_0 = 1$ and $\lambda_1 = 2$ where $a = 10, b = 20$ with $\text{ARL}_0 \approx 200$

λ	$h_2 = 4.395$ GLR CUSUM	$h_1 = 1.29$ Standardized CUSUM	$h_3 = .3237$ WLR CUSUM	$L_1 = 2.24$ EWMA-M $(r = .05)$	$L_1 = 2.45$ EWMA-M $(r = .1)$	$L_1 = 2.57$ EWMA-M $(r = .15)$	$L_1 = 2.64$ EWMA-M $(r = .2)$	$L_1 = 2.83$ EWMA-M $(r = .5)$	$L_1 = 2.80$ EWMA-1 $(r = .9)$
1.025	145.71	148.27	146.87	104.53	109.11	112.71	116.45	134.36	142.26
1.05	109.68	115.44	115.82	60.63	63.81	69.80	72.52	91.29	106.57
1.075	80.94	85.01	84.88	38.11	40.37	44.59	47.62	66.17	78.79
1.1	61.34	64.68	65.10	27.36	28.53	31.14	32.81	47.00	59.78
1.15	36.68	40.52	40.06	16.72	16.53	17.44	18.17	26.92	36.39
1.2	23.02	25.22	24.97	11.97	11.19	11.40	11.62	16.29	23.44
1.3	10.47	11.68	11.42	7.65	6.87	6.59	6.55	7.64	10.93
1.4	5.82	6.37	6.27	5.75	4.99	4.64	4.48	4.67	6.04
1.5	3.66	3.94	3.91	4.62	3.97	3.68	3.47	3.26	3.82
1.6	2.58	2.74	2.70	3.90	3.31	3.02	2.86	2.56	2.71
1.8	1.67	1.70	1.71	3.06	2.55	2.31	2.15	1.80	1.71
2	**1.29**	**1.30**	**1.31**	**2.54**	**2.11**	**1.90**	**1.78**	**1.42**	**1.31**

Table 2.A5. Comparison of ARL Values for $\lambda_0 = 1$ and $\lambda_1 = 1.2$ where $a = 10, b = 50$ with $\text{ARL}_0 \approx 200$

λ	$h_2 = 18.97$ GLR CUSUM	$h_3 = .78$ WLR CUSUM	$h_1 = 3.339$ Standardized CUSUM	$L_1 = 2.21$ EWMA-M $(r = .05)$	$L_1 = 2.43$ EWMA-M $(r = .1)$	$L_1 = 2.54$ EWMA-M $(r = .15)$	$L_1 = 2.61$ EWMA-M $(r = .2)$	$L_1 = 2.77$ EWMA-M $(r = .5)$	$L_1 = 2.75$ EWMA-1 $(r = .9)$
1.025	92.53	103.73	94.59	83.06	89.53	95.57	99.11	115.05	130.39
1.05	48.80	57.84	51.31	42.12	45.41	50.28	53.55	71.40	86.34
1.075	28.95	34.56	30.57	25.11	26.93	29.63	31.81	44.50	58.15
1.1	18.46	22.13	19.28	17.47	18.26	19.09	20.85	29.38	40.34
1.15	9.55	11.19	10.02	10.49	10.13	10.33	10.65	14.44	21.27
1.2	**6.29**	**7.43**	**6.49**	**7.41**	**6.94**	**6.90**	**6.89**	**8.40**	**12.31**
1.3	3.64	4.22	3.71	4.76	4.26	3.99	3.90	4.03	5.22
1.4	2.63	3.01	2.67	3.54	3.13	2.89	2.79	2.59	2.93
1.5	2.10	2.37	2.14	2.86	2.52	2.33	2.21	1.96	2.01
1.6	1.79	2.01	1.81	2.43	2.13	1.96	1.86	1.59	1.57
1.8	1.44	1.54	1.42	1.92	1.68	1.53	1.44	1.23	1.20
2	1.26	1.25	1.20	1.62	1.40	1.26	1.20	1.10	1.08

Table 2.A6. Comparison of ARL Values for $\lambda_0 = 1$ and $\lambda_1 = 1.5$ where $a = 10, b = 50$ with $\text{ARL}_0 \approx 200$

λ	$h_2 = 8.615$ GLR CUSUM	$h_3 = .4109$ WLR CUSUM	$h_1 = 1.562$ Standardized CUSUM	$L_1 = 2.21$ EWMA-M $(r = .05)$	$L_1 = 2.43$ EWMA-M $(r = .1)$	$L_1 = 2.54$ EWMA-M $(r = .15)$	$L_1 = 2.61$ EWMA-M $(r = .2)$	$L_1 = 2.77$ EWMA-M $(r = .5)$	$L_1 = 2.75$ EWMA-1 $(r = .9)$
1.025	125.09	139.72	130.28	83.06	89.53	95.57	99.11	115.05	130.39
1.05	78.33	98.82	86.03	42.12	45.41	50.28	53.55	71.40	86.34
1.075	52.10	67.76	58.51	25.11	26.93	29.63	31.81	44.50	58.15
1.1	33.83	47.40	39.11	17.47	18.26	19.09	20.85	29.38	40.34
1.15	16.83	24.17	19.48	10.49	10.13	10.33	10.65	14.44	21.27
1.2	9.45	13.19	11.06	7.41	6.94	6.90	6.89	8.40	12.31
1.3	4.14	5.44	4.60	4.76	4.26	3.99	3.90	4.03	5.22
1.4	2.54	3.19	2.75	3.54	3.13	2.89	2.79	2.59	2.93
1.5	**1.87**	**2.20**	**1.95**	**2.86**	**2.52**	**2.33**	**2.21**	**1.96**	**2.01**
1.6	1.52	1.76	1.56	2.43	2.13	1.96	1.86	1.59	1.57
1.8	1.22	1.28	1.20	1.92	1.68	1.53	1.44	1.23	1.20
2	1.10	1.09	1.07	1.62	1.40	1.26	1.20	1.10	1.08

Table 2.A7. Comparison of ARL Values for $\lambda_0 = 1$ and $\lambda_1 = 1.8$ where $a = 10, b = 50$ with $\text{ARL}_0 \approx 200$

λ	$h_2 = 4.593$ GLR CUSUM	$h_3 = .25$ WLR CUSUM	$h_1 = .841$ Standardized CUSUM	$L_1 = 2.21$ EWMA-M $(r = .05)$	$L_1 = 2.43$ EWMA-M $(r = .1)$	$L_1 = 2.54$ EWMA-M $(r = .15)$	$L_1 = 2.61$ EWMA-M $(r = .2)$	$L_1 = 2.77$ EWMA-M $(r = .5)$	$L_1 = 2.75$ EWMA-1 $(r = .9)$
1.025	138.76	149.58	144.84	83.06	89.53	95.57	99.11	115.05	130.39
1.05	96.81	113.92	107.38	42.12	45.41	50.28	53.55	71.40	86.34
1.075	68.21	86.19	79.08	25.11	26.93	29.63	31.81	44.50	58.15
1.1	47.89	65.41	58.00	17.47	18.26	19.09	20.85	29.38	40.34
1.15	25.64	36.66	31.64	10.49	10.13	10.33	10.65	14.44	21.27
1.2	14.72	22.06	18.68	7.41	6.94	6.90	6.89	8.40	12.31
1.3	5.96	8.59	7.47	4.76	4.26	3.99	3.90	4.03	5.22
1.4	3.12	4.17	3.69	3.54	3.13	2.89	2.79	2.59	2.93
1.5	2.05	2.58	2.33	2.86	2.52	2.33	2.21	1.96	2.01
1.6	1.57	1.80	1.68	2.43	2.13	1.96	1.86	1.59	1.57
1.8	**1.19**	**1.27**	**1.20**	**1.92**	**1.68**	**1.53**	**1.44**	**1.23**	**1.20**
2	1.07	1.08	1.07	1.62	1.40	1.26	1.20	1.10	1.08

Acknowledgment

We appreciate the helpful comments by the Editor, two referees, and Professor Douglas M. Hawkins of the University of Minnesota. This research was partially supported by NSF grant CMMI-0927323.

References

Borror, C. M.; Champ, C. W.; and Rigdon, S. E. (1998). "Poisson EWMA Control Charts". *Journal of Quality Technology* 30, pp. 352-361.

Crowder, S. V. and Hamilton, M. D. (1992). "An EWMA for Monitoring a Process Standard Deviation". *Journal of Quality Techonolgy* 24, pp. 12-21.

Dong, Y.; Hedayat, A. S.; and Sinha, B. K. (2008). "Surveillance Strategies for Detecting Changepoint in Incidence Rate Based on Exponentially Weighted Moving Average Methods". *Journal of the American Statistical Association* 103, pp. 843-853.

Ewan, W. D. and Kemp, K. W. (1960). "Sampling Inspection of Continuous Processes with No Autocorrelation Between Successive Results". *Biometrika* 47, pp. 363-380.

Frisén, M. (2009). "Optimal Sequential Surveillance for Finance, Public Health, and Other Areas". *Sequential Analysis* 28, pp. 310-337.

Frisén, M. and Sonesson, C. (2006). "Optimal Surveillance Based on Exponentially Weighted Moving Averages". *Sequential Analysis* 25, pp. 379-403.

Gan, F. F. (1990). "Monitoring Poisson Observations Using Modified Exponentially Weighted Moving Average Control Charts". *Communications in Statistics - Simulation and Computation* 19, pp. 103-124.

Hawkins, D. M. and Olwell, D. H. (1998). *Cumulative Sum Charts and Charting for Quality Improvement.* Springer, New York.

Hohle, M. and Paul, M. (2008). “Count Data Regression Charts for Monitoring of Surveillance Time Series”. *Computational Statistics and Data Analysis* 52, pp. 4357-4368.

Jensen, W. A.; Jones-Farmer, L. A.; Champ, C. W.; and Woodall, W. H. (2006). "Effects of Parameter Estimation on Control Chart Properties: A Literature Review". *Journal of Quality Technology* 38, pp. 349-364.

Knoth, S. (2009). "Discussion of 'Optimal Sequential Surveillance for Finance, Public Health, and Other Areas' by Marianne Frisén". *Sequential Analysis* 28, pp. 352-356.

Lucas, J. M. (1985). "Counted Data CUSUM's". *Technometrics* 27, pp. 129-144.

Martz, H. F. and Kvam, P. H. (1996). "Detecting Trends and Patterns in Reliability Data Over Time Using Exponentially Weighted Moving-Averages". *Reliability Engineering and System Safety* 51, pp. 201-207.

Mei, Y.; Han, S. W.; and Tsui, K. L. (2011). "Early Detection of a Change in Poisson Rate After Accounting for Population Size Effects". To appear in *Statistica Sinica*.

Montgomery, D. C. (2009). *Introduction to Statistical Quality Control, 7th Edition.* John Wiley & Sons, Inc., Hoboken, NJ.

Moustakides, G. V. (1986). "Optimal Stopping Times for Detecting Changes in Distributions". *Annals of Statistics* 14, pp. 1379-1387.

Rogerson, P. and Yamada, I. (2004). “Approaches to Syndromic Surveillance When Data Consist of Small Regional Counts”. *Morbidity and Mortality Weekly Report* 53, pp. 79-85.

Rossi, G.; Del Sarto, S.; and Marchi, M. (2010). “Approximate Poisson CUSUM Charts for the Monitoring of Time Series with Time-Varying Mean”. Proceedings of the 45th Scientific Meeting of the Italian Statistical Society (USB stick). Cleup, Padova .

Rossi, G.; Lampugnani, L.; and Marchi, M. (1999). "An Approximate CUSUM Procedure for Surveillance of Health Events". *Statistics in Medicine* 18, pp. 2111-2122.

Saniga, E. M.; Davis, D. J.; and Lucas, J. M. (2009). "Using Shewhart and CUSUM Charts for Diagnosis with Count Data in a Vendor Certification Study". *Journal of Quality Technology* 41, pp. 217-227.

Shu, L.; Jiang, W.; and Tsui, K. L. (2010). "A Comparison of Weighted CUSUM Procedures that Account for Monotone Changes in Population Size". *Statistics in Medicine*, n/a. doi: 10.1002/sim.4122.

Weiss, C. H. and Testik, M. C. (2009). "CUSUM Monitoring of First-Order Integer-Valued Autoregressive Processes of Poisson Counts". *Journal of Quality Technology* 41, pp. 389-400.

Woodall, W. H. and Mahmoud, M. A. (2005). "The Inertial Properties of Quality Control Charts". *Technometrics* 47, pp. 425-436.

Yashchin, E. (1989). "Weighted Cumulative Sum Technique". *Technometrics* 31, pp. 321-338.

Chapter 3

Methods for Monitoring Multiple Proportions When Inspecting Continuously

ANNE G. RYAN, LEE J. WELLS and WILLIAM H. WOODALL

Virginia Tech, Blacksburg, VA 24061-0439

As technology advances, the need for methods to monitor processes that produce readily available inspection data becomes essential. In this paper a multinomial cumulative sum (CUSUM) chart is proposed to monitor in situations where items can be classified into more than two categories, the items are not put into subgroups, and the direction of the out-of-control shift in the parameter vector can be specified. It is shown through examples that the multinomial CUSUM chart can detect shifts in category probabilities at least as quickly, and in most cases faster, than using multiple Bernoulli CUSUM charts. The properties of the multinomial CUSUM chart are determined through a Markov chain representation. If the direction of the out-of-control shift in the parameter vector cannot be specified, we recommend the use of multiple Bernoulli CUSUM charts.

Key Words: Average Run Length, Bernoulli Cumulative Sum Chart, Grouped Data, Multinomial Distribution, Statistical Process Control.

Ms. Ryan is a Ph.D. candidate in the Department of Statistics. Her e-mail address is agryan@vt.edu.

Mr. Wells is a Ph.D. candidate in the Grado Department of Industrial and Systems Engineering. His email is leejay@vt.edu.

Dr. Woodall is a Professor in the Department of Statistics. He is a Fellow of ASQ. His e-mail address is bwoodall@vt.edu.

Introduction

When choosing a process monitoring technique, one of the first requirements is to consider the type of data being measured. Attribute data, such as counts or pass/fail-type data, are collected in many healthcare and industrial applications. For example, one might have manufactured parts that are classified as either conforming or nonconforming. The objective would be to detect changes in the proportion of nonconforming components. This situation is an example of monitoring with attribute data, reviews of which were provided by Woodall (1997) and Topalidou and Psarakis (2009).

The traditional approach for monitoring the fraction of nonconforming items, p, is to use the Shewhart *p*-chart, which plots the proportion of nonconforming items for each sample. An alternative to the *p*-chart is the binomial cumulative sum (CUSUM) chart. Gan (1993) discussed the construction of the binomial CUSUM chart where the plotted CUSUM statistics are based on the proportion of nonconforming items for each sample. However, suppose a process that is being monitored produces a continuous stream of inspection data leading to immediately available information. Because the binomial CUSUM chart and the *p*-chart are both based on the proportion of nonconforming items for specified samples of sizes $n > 1$, the monitoring process must wait until the required number of inspected items can be aggregated. As a result, *p*-charts and binomial CUSUM charts have an inherent delay in detecting shifts in the underlying proportion, which causes slower detection of process changes and a loss of information regarding when shifts occur.

Reynolds and Stoumbos (1999) proposed using a Bernoulli CUSUM chart to take advantage of readily available inspection data. The Bernoulli CUSUM chart is a special case of the binomial CUSUM chart when $n = 1$. Because each sampling point for the Bernoulli CUSUM chart consists of a single observation, Reynolds and Stoumbos (1999) used the average number of observations to signal (ANOS) in place of the average run length (ARL) for easier comparisons to charts based on sample proportions with $n > 1$. In our paper, we will use the term ARL instead of ANOS since all of the methods we compare have $n = 1$. Reynolds and Stoumbos (1999) compared the ANOS performance of the Bernoulli CUSUM chart with the Shewhart *p*-chart and the binomial CUSUM chart. They found that Bernoulli CUSUM charts

will detect shifts in p much faster (on average) compared to both p-charts and binomial CUSUM charts in situations where there is a continuous stream of inspection data.

Reynolds and Stoumbos (1999) discussed the two-sided Bernoulli CUSUM chart; however, they focused on the one-sided Bernoulli CUSUM chart where the objective is to detect an increase in the proportion of nonconforming items, p, reflecting a decrease in the quality of the process. The Bernoulli CUSUM chart given in Reynolds and Stoumbos (1999) is based on the CUSUM likelihood ratio formulation. We let X_1, X_2, ... be a sequence of independent Bernoulli random variables, where

$$X_t = \begin{cases} 1 & \text{if the } t^{th} \text{ item is nonconforming} \\ 0 & \text{otherwise} \end{cases}, t = 1, 2, \ldots .$$

It is assumed that p_0 is the in-control probability of a nonconforming item and p_1 is the out-of-control probability of a nonconforming item of interest to detect quickly. The Bernoulli CUSUM statistics are

$$S_t = \max(0, S_{t-1} + L_t), t = 1, 2, \ldots , \tag{1}$$

where $S_0 = 0$. The values for the log-likelihood scores, L_t, in the form given by Steiner et al. (2000) are

$$L_t = \begin{cases} \ln\left(\frac{1-p_1}{1-p_0}\right) & \text{if } X_t = 0 \\ \ln\left(\frac{p_1}{p_0}\right) & \text{if } X_t = 1 \end{cases} . \tag{2}$$

The chart signals if $S_t > h$, where the decision limit h is determined based on a specified value of the in-control ARL, ARL_0.

The p-chart, binomial CUSUM chart, and Bernoulli CUSUM chart can all be used to monitor the proportion of nonconforming items. However, suppose that instead of classifying items as conforming or nonconforming, the items are now being classified into more categories, e.g., conforming, minor nonconforming, and major nonconforming. An example of multiple classifications is seen in the inspection of clothing. A garment with no flaws is classified as "conforming" and sent to the retailer to be sold at full price. A garment with a limited number of minor flaws is classified as "seconds" and is sent to an outlet store to be sold at a discount, while a garment classified as "defective" is scrapped. There are other situations where binary outcomes can be extended to more than two categories. Steiner et al. (2000) focused on a 30-day post-

operative mortality rate. Suppose that instead of considering only whether a patient lives or dies after surgery, it is of interest whether the patient lives, develops a major complication, or dies in the thirty days following the procedure. The outcome of interest has now been extended to three categories rather than two, which leads to additional information regarding the condition of the patients after surgery. With multiple categories of classification, the process no longer produces Bernoulli or binomial random variables; but instead produces multinomial random variables. A review of multinomial and multiattribute quality control charts was given by Topalidou and Psarakis (2009).

In the next section we describe a CUSUM procedure for multinomial data without subgrouping. The method is very similar to the use of CUSUM charts with grouped data as discussed by Steiner et al. (1996a). It can also be viewed as an attribute version of the CUSUM method of Healy (1987), who used a univariate CUSUM method with multivariate normal data when the direction of the shift in the mean vector could be specified.

Following the derivation of the multinomial CUSUM chart, the zero-state ARL performance of the multinomial CUSUM chart with three categories and multiple Bernoulli CUSUM charts is compared through a simulation study. Next, the multinomial CUSUM chart with four categories is discussed, and then the general form of the multinomial CUSUM chart for $n > 1$ is given. This is followed by a section exploring the effects on the zero-state ARL performance of the multinomial CUSUM chart when the shift direction of the parameter vector is misspecified. Finally, we discuss the practical issues associated with multinomial control charting without subgrouping along with some extensions and conclusions. Technical details about the Markov chain representation used to calculate exact ARL values for the multinomial CUSUM chart are given in the appendix. Additional comparisons for trinomial processes and steady-state ARL analyses are also given in the appendix.

Multinomial Control Charts

One approach for monitoring processes when items fall into multiple categories is to use a *p*-chart for each category. Duncan (1950) realized that as the number of categories increases, the use of multiple *p*-charts can become cumbersome. Thus Duncan (1950) advised using a control chart based on the chi-square distribution to monitor processes where items can be classified into

several categories, instead of using multiple *p*-charts. Marcucci (1985) and Nelson (1987) also considered the chi-square control chart.

Tucker et al. (2002) studied control charts for ordinal data. They proposed a control chart for monitoring a process with ordinal data that is based on the maximum likelihood estimates (MLEs) of the parameters of an assumed underlying, but unobservable, continuous distribution that was used to determine the probabilities associated with the various categories. Tucker et al. (2002) compared charts based on different underlying quality distributions with the chi-square control chart and found that control charts based on the MLEs were much better at detecting improvements in quality. They also found that the MLE control charts with a normal or logistic underlying distribution performed as well or better than the chi-square chart at detecting deterioration in quality.

One common requirement of these control charts for multinomial random variables is that the observations be aggregated into samples. Again, the question rises concerning what is the best method for monitoring a process that produces a continuous stream of data where inspection results are immediately available. The argument by Reynolds and Stoumbos (1999), that signaling of process changes will be delayed if one must wait for samples to be taken before a control chart statistic can be computed, continues to hold when monitoring multinomial data. This situation motivates the use of a multinomial CUSUM chart where $n = 1$, which is a generalization of Reynolds and Stoumbos' (1999) Bernoulli CUSUM chart.

In industry there are situations where "grouping" a continuous variable is more practical because it may be easier, faster, or less expensive than obtaining a more exact measurement. The idea of monitoring processes where a continuous variable is classified into intervals or "groups" was extensively studied in Steiner et al. (1994), Steiner et al. (1996a,b), and Steiner (1998), where one does not take a continuous measurement on an item. Instead one only obtains enough information to classify the value of the quality characteristic into one of several groups, each defined by upper and lower limits. Steiner et al. (1994) proposed a *k*-step-gauge control chart that uses grouped observations to detect shifts in the mean of a normal distribution. Steiner et al. (1996b) suggested a *k*-step-gauge Shewhart control chart based on grouped observations for monitoring the mean and standard deviation of a process. Steiner (1998) proposed a *k*-group EWMA control chart which accommodates data that has been classified into groups. It is shown through ARL comparisons that the *k*-group EWMA control chart is nearly as efficient as the

EWMA control chart based on continuous observations for small mean shifts of interest. Steiner et al. (1996a) advocated using a CUSUM chart based on multinomial likelihoods for monitoring observations that are classified into groups.

The multinomial CUSUM chart approach in Steiner et al. (1996a) is very similar to the multinomial CUSUM chart approach being proposed in our paper. However, the data studied by Steiner et al. (1996a) involved a continuous variable classified into groups. Therefore, the data and category probabilities have a structure that is determined by the underlying continuous distribution. The data being studied in our paper are attribute data, where no underlying continuous distribution exists. We could assume a hypothetical underlying continuous distribution, as in Tucker et al. (2002), to determine the out-of-control category probabilities if the categories are ordinal, but we do not do so. While our CUSUM procedure matches that proposed by Steiner et al. (1996a), the main differences lie in the distinction between the types of data and the increased flexibility in the design of our multinomial approach since the probabilities do not depend on any underlying distribution. In addition, we do not believe that it is generally recognized that the grouped data method applies with attribute data when there is no grouping of a continuous variable involved or when the categories are not ordered.

We let $X_1, X_2,$ ... be a sequence of independent multinomial random variables, where

$X_t = i$ if the t^{th} item is classified in the i^{th} category, $t = 1, 2, ..., i = 1, 2, ..., k.$ (3)

Also, we let $p_{0,i}$ and $p_{1,i}$ be the in-control and out-of-control probability of being classified into category i for $i = 1, 2, ..., k$, respectively, where $\sum_{i=1}^{k} p_{0,i} = 1$ and $\sum_{i=1}^{k} p_{1,i} = 1$. Like the Bernoulli CUSUM chart, the multinomial CUSUM chart is based on the CUSUM likelihood-ratio formulation. The multinomial CUSUM statistics are

$$S_t = \max(0, S_{t-1} + L_t), t = 1, 2, ... \quad (4)$$

where $S_0 = 0$ and L_t is the log-likelihood ratio score for $t = 1, 2, ...$. The values of L_t are

$$L_t = \ln\left(\frac{p_{1,i}}{p_{0,i}}\right) \text{ when } X_t = i, i = 1, 2, ..., k, t = 1, 2, ... \quad (5)$$

The chart signals if $S_t > h_m$, where the value h_m is determined based on the specified value of ARL_0. When designing the multinomial CUSUM chart, it is important to examine the ratio of in-control probabilities to out-of-control probabilities for the categories. If any of these ratios are

the same then the corresponding categories can be combined. This feature was also discussed in Steiner et al. (1996a) for the grouped data CUSUM chart.

Since the aggregation of items into samples is not required, the multinomial CUSUM chart should quickly detect shifts in the category probabilities as long as the probabilities change in the anticipated direction as specified by the $p_{1,i}$ values. Another alternative is to use multiple Bernoulli CUSUM charts to monitor the process. A simulation study is given in the next section which compares the ARL performance for the multinomial CUSUM chart against the simultaneous use of multiple Bernoulli CUSUM charts.

Multinomial CUSUM and Bernoulli CUSUM Chart Comparisons

Three cases are explored in this section to illustrate the usefulness of the multinomial CUSUM chart compared to using separate Bernoulli CUSUM charts. All three cases involve a process where components can be classified in one of the following three categories: good, fair, and bad. The methods would apply exactly the same, however, if the categories were unordered and listed simply as A, B, and C. The statistics of the multinomial CUSUM chart incorporate the three probabilities of classification. An alternative method for monitoring a process with multiple categories is to use a combination of Bernoulli CUSUM charts. One could use a Bernoulli CUSUM chart where either $k-1$ Bernoulli CUSUM charts or k Bernoulli CUSUM charts are run simultaneously. For a process with three categories, the three categories must be combined into two categories to use Bernoulli CUSUM charts for monitoring. This leads to three possible Bernoulli CUSUM charts, a Bernoulli CUSUM chart that focuses on the good category, a Bernoulli CUSUM chart that focuses on the fair category, and a Bernoulli CUSUM chart that focuses on the bad category. From these three Bernoulli CUSUM charts we choose two charts to run simultaneously and refer to this chart as the 2-Bernoulli CUSUM chart. Even though there are three parameters, intuitively one would think only two charts are necessary since the three proportions of interest must sum to one. However, there are three possible 2-Bernoulli CUSUM charts. For the sake of completeness we also study the simultaneous Bernoulli CUSUM method that consists of all three Bernoulli charts, i.e., the 3-Bernoulli CUSUM chart.

The multinomial CUSUM chart and simultaneous Bernoulli CUSUM charts are compared based on their ARL values. The zero-state ARL values for the multinomial CUSUM chart were found using a Markov chain representation and the zero-state ARL values for the simultaneous

Bernoulli CUSUM charts were found using simulation. Steady-state ARL comparisons for all three cases are given in Appendix D. The multinomial CUSUM chart also had nice ARL performance in the steady-state ARL analyses. A detailed explanation of our Markov chain representation can also be found in the appendix.

For our examples we considered three different cases for the design of the competing charts. The properties of the simultaneous Bernoulli CUSUM charts for Cases 1 and 2 were found using simulations, where each estimated ARL value was estimated using 100,000 simulations, while the ARL values for Case 3 were estimated using 1 million simulations. In order to obtain the upper control limits for simultaneous pairs of Bernoulli CUSUM charts, we first found control limits that resulted in individual Bernoulli CUSUM charts with ARL_0 values of two times the desired ARL_0 value for the simultaneous Bernoulli CUSUM chart. We will refer to these upper control limits as h_g, h_f, and h_b for the Bernoulli CUSUM charts that focus on the good, fair, and bad categories, respectively. After the values of the upper control limits were determined for the individual charts, two of the three Bernoulli charts were run simultaneously and the upper control limits were slightly adjusted in order to achieve the desired overall value of ARL_0 more closely. A similar approach was used to find the control limits for the 3-Bernoulli CUSUM chart.

The first case studied has the largest in-control and out-of-control probabilities for fair and bad components, compared to the other two cases. These probabilities are displayed in Table 3.1. Here we are concerned with detecting a decrease in the probability of good components, and increases in the probabilities of fair and bad components. Table 3.1 also contains adjusted out-of-control probabilities, which are the probabilities that were adjusted slightly so that the Markov chain could be used to obtain exact ARL values for the multinomial CUSUM chart. A more detailed discussion of these adjustments can be found in the Appendix A.

Table 3.1. Probabilities for Case 1

Categories	Good (1)	Fair (2)	Bad (3)
In-Control	0.65	0.25	0.10
Out-of-Control	0.45	0.30	0.25
Adjusted Out-of-Control	0.4517	0.2999	0.2484

For Case 1, the ARL comparisons of the multinomial CUSUM chart and the simultaneous Bernoulli CUSUM charts are shown in Table 3.2. In all ARL comparison tables, the smallest ARL value appears in italicized font. It should be noted that the choice of which two Bernoulli CUSUM charts to run simultaneously impacts the performance of the 2-Bernoulli CUSUM chart. Among the three 2-Bernoulli CUSUM charts, the best performing chart (for the majority of shifts) is the chart that focuses on both the good and bad categories. The 2-Bernoulli CUSUM chart that focuses on the good and fair categories begins to have better ARL performance for large shifts. However, the multinomial CUSUM chart which incorporates the information from the three categories outperforms all of the simultaneous Bernoulli CUSUM charts for all probability shifts considered.

The multinomial and simultaneous Bernoulli CUSUM charts are optimized for the probabilities indexed as Distribution 6. The ARL value for the multinomial CUSUM chart is 21.57 while the corresponding ARL value of the 2-Bernoulli CUSUM chart which focuses on the good and bad categories is 24.03 for this distribution. The multinomial CUSUM chart also has quicker detection for both smaller and larger shifts, indicating that the multinomial CUSUM chart is preferred over the simultaneous Bernoulli CUSUM charts for Case 1 as long as the shifts in the category probabilities are in the direction for which the chart was designed.

The 3-Bernoulli CUSUM chart has slower detection of parameter shifts compared to the multinomial CUSUM chart and the best performing 2-Bernoulli CUSUM chart. However, if one chooses to use a simultaneous Bernoulli CUSUM chart instead of the multinomial CUSUM chart, we recommend using the 3-Bernoulli CUSUM chart. Even though there is some delay in detection when using the 3-Bernoulli CUSUM chart, it is more difficult to determine the best performing 2-Bernoulli CUSUM chart out of the three possible charts.

Table 3.2. Zero-State ARL Comparisons for Case 1

Distribution	p_1 P(Good)	p_2 P(Fair)	p_3 P(Bad)	Multinomial CUSUM ARL $h_m = 2.95$	2-Bernoulli CUSUM ARL $h_g = 3.72$ $h_b = 3.10$	2-Bernoulli CUSUM ARL $h_f = 1.712$ $h_b = 3.332$	2-Bernoulli CUSUM ARL $h_g = 2.93$ $h_f = 2.71$	3-Bernoulli CUSUM ARL $h_g = 3.706$ $h_f = 1.7896$ $h_b = 3.506$
1 (in-control)	0.65	0.25	0.10	279.96	282.38	280.48	280.07	281.00
2	0.625	0.255	0.12	*153.82*	155.35	174.79	178.67	171.06
3	0.60	0.26	0.14	*95.54*	97.15	114.72	121.52	110.74
4	0.55	0.27	0.18	*47.45*	49.37	59.72	64.63	56.38
5	0.50	0.28	0.22	*29.29*	31.40	38.01	40.24	35.51
6	**0.4517**	**0.2999**	**0.2484**	***21.57***	**24.03**	**29.29**	**28.42**	**26.78**
7	0.35	0.35	0.30	*14.26*	16.22	20.27	17.11	17.70
8	0.25	0.40	0.35	*10.58*	12.33	15.57	12.18	13.23
9	0.15	0.45	0.40	*8.40*	9.93	12.59	9.47	10.57
10	0.05	0.50	0.45	*6.95*	8.34	10.60	7.70	8.87

The in-control and out-of-control probabilities for the fair and bad categories in Case 2 are slightly smaller than those seen in Case 1. The probabilities for Case 2 are given in Table 3.3. Again, we are examining a case where we are interested in detecting an increase in the probabilities of fair and bad components and a decrease in the probability of good components.

Table 3.3. Probabilities for Case 2

Categories	Good (1)	Fair (2)	Bad (3)
In-Control	0.94	0.05	0.01
Out-of-Control	0.85	0.10	0.05
Adjusted Out-of-Control	0.8495	0.0992	0.0513

The ARL results for Case 2, displayed in Table 3.4, are similar to those seen in Case 1. Not only does the multinomial CUSUM chart have better ARL performance compared to the simultaneous Bernoulli CUSUM charts for the optimized shift indexed as Distribution 5, the multinomial CUSUM chart also has quicker detection for all other shifts considered. As in Case 1, the best performing simultaneous Bernoulli CUSUM chart in Case 2 for most shifts in the distribution is the 2-Bernoulli CUSUM chart that focuses on the good and bad categories, while

the 2-Bernoulli CUSUM chart that focuses on the good and fair categories has better performance for some large shifts.

Table 3.4. Zero-State ARL Comparisons for Case 2

Distribution	p_1 P(Good)	p_2 P(Fair)	p_3 P(Bad)	Multinomial CUSUM ARL $h_m = 2.80$	2-Bernoulli CUSUM ARL $h_g = 3.375$ $h_b = 2.8295$	2-Bernoulli CUSUM ARL $h_f = 2.734$ $h_b = 2.9055$	2-Bernoulli CUSUM ARL $h_g = 3.12$ $h_f = 2.36$	3-Bernoulli CUSUM ARL $h_g = 3.6288$ $h_f = 2.8288$ $h_b = 2.9288$
1 (in-control)	0.94	0.05	0.01	500.61	502.88	501.23	499.20	505.39
2	0.925	0.06	0.015	*230.68*	233.77	238.20	251.06	236.31
3	0.89	0.08	0.03	*74.35*	77.25	83.43	92.41	81.02
4	0.87	0.09	0.04	*49.69*	52.51	58.03	64.01	55.72
5	**0.8495**	**0.0992**	**0.0513**	***36.21***	**38.81**	**43.44**	**47.47**	**41.49**
6	0.80	0.15	0.05	*26.41*	27.62	31.38	28.11	29.12
7	0.74	0.20	0.06	*18.33*	19.07	22.13	18.85	20.27
8	0.60	0.30	0.10	*10.12*	10.86	12.72	10.73	11.57
9	0.50	0.35	0.15	*7.36*	8.05	9.46	8.25	8.60
10	0.40	0.40	0.20	*5.79*	6.36	7.48	6.72	6.84

In the last case, Case 3, the in-control and out-of-control probabilities for the fair and bad components given in Table 3.5 are very small, resulting in a process that produces mostly good components. The ARL values for Case 3 are given in Table 3.6. The ARL values for both the multinomial CUSUM chart and 2-Bernoulli CUSUM chart that focuses on the good and bad categories are virtually the same for Case 3. This means there seems to be little advantage in using the multinomial CUSUM chart when the probability of having a fair or bad component is very small. Additional comparisons of ARL performance for trinomial processes are given in Appendix C.

Table 3.5. Probabilities for Case 3

Categories	Good (1)	Fair (2)	Bad (3)
In-Control	0.994	0.005	0.001
Out-of-Control	0.985	0.01	0.005
Adjusted Out-of-Control	0.9848	0.0099	0.0053

Table 3.6. Zero-State ARL Comparisons for Case 3

Distribution	p_1 P(Good)	p_2 P(Fair)	p_3 P(Bad)	Multinomial CUSUM ARL h_m =0.8337	2-Bernoulli CUSUM ARL $h_g = 1.335$ $h_b = 0.0032$	2-Bernoulli CUSUM ARL $h_f = 1.13$ $h_b = 0.004$	2-Bernoulli CUSUM ARL $h_g = 0.928$ $h_f = 0.865$	3-Bernoulli CUSUM ARL $h_g = 1.60$ $h_f = 1.13$ $h_b = 1.38$
1 (in-control)	0.994	0.005	0.001	499.64	498.29	499.94	526.70	499.94
2	0.99	0.0075	0.0025	227.69	*226.91*	227.86	254.74	227.86
3	0.987	0.009	0.004	155.02	*154.77*	155.81	181.03	155.81
4	**0.9848**	**0.0099**	**0.0053**	**124.44**	***124.33***	**125.32**	**149.21**	**125.32**
5	0.98	0.015	0.005	98.43	*98.38*	99.46	107.20	99.46
6	0.974	0.02	0.006	*73.72*	73.82	74.77	79.59	74.77
7	0.96	0.03	0.01	*45.09*	45.15	45.65	50.40	45.65
8	0.95	0.035	0.015	34.49	*34.48*	34.75	40.11	34.75
9	0.94	0.04	0.02	27.97	*27.95*	28.09	33.33	28.09
10	0.90	0.06	0.04	*16.01*	*16.01*	*16.01*	20.01	*16.01*
11	0.85	0.09	0.06	*10.67*	*10.67*	*10.67*	13.33	*10.67*
12	0.80	0.11	0.09	*7.75*	*7.75*	*7.75*	10.00	*7.75*
13	0.70	0.17	0.13	*5.22*	*5.22*	*5.22*	6.66	*5.22*
14	0.60	0.24	0.16	*4.00*	*4.00*	*4.00*	5.00	*4.00*
15	0.50	0.30	0.20	*3.20*	*3.20*	*3.20*	4.00	*3.20*
16	0.30	0.40	0.30	*2.24*	*2.24*	2.25	2.86	2.25

A Multinomial Process with Four Categories

As the number of classification categories increases, the complications associated with the use of simultaneous Bernoulli CUSUM charts escalate. These complications are illustrated through Case 4, a multinomial process with four classification categories. The probabilities for Case 4 are displayed in Table 3.7.

Table 3.7. Probabilities for Case 4

Categories	1	2	3	4
In-Control	0.65	0.20	0.10	0.05
Out-of-Control	0.40	0.325	0.175	0.10
Adjusted Out-of-Control	0.3960	0.3283	0.1734	0.1023

An advantage of the multinomial CUSUM chart is there is only one control limit, h, that must be determined regardless of the number of categories. As the number of categories increases, the possible combinations of Bernoulli CUSUM charts increases, as does the number of control limits that must be determined. Also, the different combinations of Bernoulli CUSUM charts can have considerably different performance, even though the charts may have the same in-control ARL. It seems reasonable to use combinations of three-Bernoulli CUSUM charts or to use all four, i.e., the 3-Bernoulli CUSUM chart or the 4-Bernoulli CUSUM chart. We studied all four 3-Bernoulli CUSUM charts and the 4-Bernoulli CUSUM chart for Case 4. The ARL values were obtained from 100,000 simulations.

The results for Case 4, given in Table 3.8, are similar to the results in Case 1. The multinomial CUSUM chart has better ARL performance compared to all five combinations of the simultaneous Bernoulli CUSUM charts studied. Among the simultaneous Bernoulli CUSUM charts, the 3-Bernoulli CUSUM chart focusing on categories 1, 3, and 4 has quickest detection for small shifts and the 3-Bernoulli CUSUM chart that focuses on categories 1, 2, and 3 has the quickest detection for the larger shifts. The average detection time for the 4-Bernoulli CUSUM chart is only slightly delayed compared to the best performing 3-Bernoulli CUSUM chart for each parameter shift of interest.

Case 4 illustrates that the multinomial CUSUM chart exhibits good performance when the shift is in the direction for which the chart was designed. If the shift direction cannot be specified, then we recommend using the 4-Bernoulli CUSUM chart. Even though different combinations of Bernoulli CUSUM charts may have better ARL performance, as seen in Case 4, it is difficult to choose and design the best performing chart without a simulation study.

Table 3.8. Zero-State ARL Comparisons for Case 4

Distribution	p_1	p_2	p_3	p_4	Multinomial CUSUM ARL $h_m = 3.25$	3-Bernoulli CUSUM ARL $h_1 = 4.12$ $h_2 = 3.20$ $h_4 = 2.49$	3-Bernoulli CUSUM ARL $h_1 = 3.87$ $h_2 = 3.31$ $h_3 = 2.80$	3-Bernoulli CUSUM ARL $h_1 = 3.98$ $h_3 = 2.82$ $h_4 = 2.62$	3-Bernoulli CUSUM ARL $h_2 = 3.35$ $h_3 = 2.86$ $h_4 = 2.66$	4-Bernoulli CUSUM ARL $h_1 = 4.575$ $h_2 = 3.43$ $h_3 = 2.93$ $h_4 = 2.73$
1 (in-control)	0.65	0.20	0.10	0.05	286.99	279.76	282.59	281.83	282.13	285.19
2	0.60	0.22	0.12	0.06	*125.94*	138.02	128.83	127.10	137.30	133.07
3	0.55	0.24	0.14	0.07	*66.71*	78.47	71.64	71.07	82.77	76.82
4	0.50	0.26	0.16	0.08	*40.92*	50.04	45.86	45.85	57.14	50.63
5	0.46	0.28	0.17	0.09	*30.00*	36.95	34.71	34.90	45.88	38.89
6	**0.3960**	**0.3283**	**0.1734**	**0.1023**	***20.56***	**25.25**	**24.05**	**24.74**	**34.71**	**27.67**
7	0.35	0.34	0.19	0.12	*16.37*	20.39	19.45	19.90	29.35	22.39
8	0.30	0.35	0.21	0.14	*13.33*	16.85	15.99	16.35	25.14	18.53
9	0.25	0.36	0.23	0.16	*11.22*	14.24	13.60	13.93	21.86	15.75
10	0.20	0.38	0.24	0.18	*9.70*	12.30	11.85	12.13	19.39	13.71
11	0.15	0.40	0.25	0.20	*8.53*	10.78	10.56	10.72	17.43	12.09
12	0.10	0.42	0.26	0.22	*7.62*	9.58	9.56	9.59	15.81	10.78
13	0.05	0.43	0.28	0.24	*6.87*	8.64	8.74	8.63	14.47	9.68

Extension of the Multinomial CUSUM Chart to Samples of Size $n > 1$

The multinomial CUSUM procedure described in Equation (3), Equation (4), and Equation (5) can be generalized to include samples of size $n > 1$ as outlined by Steiner et al. (1996a). For a sample where $m_1, \ldots, m_k$ correspond to the numbers of observations in each of the k categories, the multinomial CUSUM statistics can be defined as

$$S_t = \max(0, S_{t-1} + L_t), t = 1, 2, \ldots \quad (6)$$

where $S_0 = 0$ and L_t is the log-likelihood ratio score for $t = 1, 2, \ldots$. The values of L_t are

$$L_t = \sum_{i=1}^{k} m_i \ln\left(\frac{p_{1,i}}{p_{0,i}}\right), \quad (7)$$

where k is the total number of categories. The multinomial CUSUM chart signals when $S_t > h$, where the decision limit, h, can be determined by simulation.

Effects of Misspecified Parameter Shifts

The results thus far have indicated that the multinomial CUSUM chart performs just as well or better than Bernoulli CUSUM charts for monitoring multinomial processes when the shifts in the probabilities are in the anticipated direction. This begs the question of what are the effects on chart performance when the shifts in parameters are not in the anticipated directions or the shift direction is unknown. For these situations, we recommend using the k-Bernoulli CUSUM chart for monitoring rather than the multinomial CUSUM chart.

In order to explore the effects of misspecifed parameter shifts, we studied two cases where modifications were made to Case 1. For both cases, the multinomial CUSUM chart and simultaneous Bernoulli CUSUM charts were designed to detect shifts in the probabilities as given in Table 3.1. In Case 1, the charts were designed to detect decreases in the probability of good components, but in this study, Case A, the probabilities of good components increase. The charts were also designed to detect increases in the probability of fair components, but the actual probabilities of fair components for Case A decrease.

The results of the study of misspecification for Case A are given in Table 3.9. The comparisons reveal that the 2-Bernoulli CUSUM chart that focuses on both the good and bad categories outperforms the other combinations of simultaneous Bernoulli CUSUM charts and the multinomial CUSUM chart when the probabilities shift in directions for which the chart was not designed to detect.

The second case, Case B, considers various parameter shifts in misspecified directions, which are displayed in Table 3.10. This case illustrates the weakness of the multinomial CUSUM chart for detecting shifts in misspecified directions. In Distribution 2 all three probabilities shift in the opposite direction compared to the shift direction the multinomial CUSUM chart was designed to detect. The multinomial CUSUM chart ARL for this parameter shift is 1081.05 compared to the 2-Bernoulli CUSUM chart that focuses on the good and fair categories which has an ARL of 825.36. This illustrates that if one would like to detect improvements in the process, then a two-sided CUSUM chart is needed for monitoring. Also, among the 2-Bernoulli CUSUM charts, different charts perform considerably better than others for different shifts. In situations when the shift direction is unknown, it becomes difficult to choose the best 2-Bernoulli

CUSUM chart. Even though the 3-Bernoulli CUSUM chart does not have the best performance for each of the parameter shifts in Case B, the 3-Bernoulli CUSUM chart has comparable performance with the best 2-Bernoulli CUSUM chart. Therefore, for situations when the probability shifts cannot be specified or one is concerned that the probabilities may not shift in the specified direction, we recommend using the 3-Bernoulli CUSUM chart. Detection may be delayed to some extent compared to other combinations of Bernoulli CUSUM charts, but regardless of the number of categories there is only one k-Bernoulli CUSUM chart to consider and design. Other examples of misspecified shifts could be considered, but generally we would expect the performance of the multinomial CUSUM chart to be adversely affected.

Table 3.9. Zero-State ARL Comparisons for Misspecified Parameter Shifts for Case A

Distribution	p_1 P(Good)	p_2 P(Fair)	p_3 P(Bad)	Multinomial CUSUM ARL $h_m = 2.95$	2-Bernoulli CUSUM ARL $h_g = 3.72$ $h_b = 3.10$	2-Bernoulli CUSUM ARL $h_f = 1.712$ $h_b = 3.332$	2-Bernoulli CUSUM ARL $h_g = 2.93$ $h_f = 2.71$	3-Bernoulli CUSUM ARL $h_g = 3.706$ $h_f = 1.7896$ $h_b = 3.506$
1 (in-control)	0.65	0.25	0.10	279.96	282.38	280.48	280.07	281.00
2	0.66	0.22	0.12	193.53	*184.30*	235.12	343.98	244.93
3	0.67	0.20	0.13	170.57	*148.45*	190.28	425.50	204.23
4	0.68	0.18	0.14	152.01	*120.50*	149.29	529.12	163.29
5	0.69	0.15	0.16	117.63	*81.37*	97.18	663.35	106.13
6	0.72	0.10	0.18	104.19	*59.06*	68.09	1416.74	74.23
7	0.73	0.07	0.20	85.56	*45.46*	51.54	1868.80	55.56
8	0.74	0.05	0.21	79.98	*40.48*	45.71	2497.37	48.98
9	0.75	0.02	0.23	67.91	*32.95*	36.99	3374.39	39.37

Table 3.10. Zero-State ARL Comparisons for Misspecified Parameter Shifts for Case B

Distribution	p_1 P(Good)	p_2 P(Fair)	p_3 P(Bad)	Multinomial CUSUM ARL $h_m = 2.95$	2-Bernoulli CUSUM ARL $h_g = 3.72$ $h_b = 3.10$	2-Bernoulli CUSUM ARL $h_f = 1.712$ $h_b = 3.332$	2-Bernoulli CUSUM ARL $h_g = 2.93$ $h_f = 2.71$	3-Bernoulli CUSUM ARL $h_g = 3.706$ $h_f = 1.7896$ $h_b = 3.506$
1 (in-control)	0.65	0.25	0.10	279.96	282.38	280.48	280.07	281.00
2	0.70	0.23	0.07	1081.05	1122.26	827.42	*825.36*	879.27
3	0.80	0.09	0.11	628.67	*279.88*	374.85	19420.49	445.12
4	0.68	0.23	0.09	*460.61*	469.48	506.52	522.95	527.15
5	0.60	0.32	0.08	317.04	194.82	*105.36*	109.90	105.41
6	0.70	0.19	0.11	315.55	*269.60*	365.08	843.63	405.01
7	0.50	0.45	0.05	298.7	55.80	*37.75*	38.47	37.83
8	0.45	0.15	0.40	12.80	*12.50*	13.53	28.24	14.24
9	0.40	0.20	0.40	*11.81*	12.34	13.51	21.38	14.04

Conclusions

There are many practical situations where categorical data are collected over time and these data have no underlying continuous distributions. The multinomial CUSUM chart is an extension of the Bernoulli CUSUM chart that uses all the information given by this type of data. In contrast to combining probabilities to create two categories as would be done when using multiple Bernoulli CUSUM charts, the number of categories is preserved when multinomial CUSUM charts are used since the statistics are based on the probabilities of being in each category. The examples explored in our paper reveal that the multinomial CUSUM charts performed just as well or better than the simultaneous Bernoulli CUSUM charts when the shifts in the probabilities are in the anticipated direction. Also, the multinomial CUSUM chart only requires one upper control limit to be determined, compared to multiple upper control limits if Bernoulli CUSUM charts are implemented.

If one wants to detect shifts in the category probabilities in any direction, then the k-Bernoulli CUSUM chart would be preferred, where each of the k Bernoulli CUSUM charts focus

on one of the k categories. We choose this approach compared to other combinations of Bernoulli CUSUM charts because of the difficulty associated with choosing the best combination of Bernoulli CUSUM charts without performing a simulation study. The k-Bernoulli CUSUM chart is also the preferred method for monitoring in situations when one believes that the probabilities may shift in unanticipated directions because the use of the k-Bernoulli CUSUM chart avoids some of the worst ARL performance that is associated with various simultaneous Bernoulli CUSUM charts and the multinomial CUSUM chart. Determination of further guidelines for the choice of the best performing Bernoulli CUSUM charts for multinomial processes is an objective for future studies.

We have shown through examples that there are added benefits if a multinomial CUSUM chart is used when there are three or four categories. It is expected that these results could extend to situations where the multinomial process has any number of categories. It would also be of interest to investigate risk-adjustment with the multinomial CUSUM control chart as done by Steiner et al. (2000) with the Bernoulli CUSUM control chart. Other areas of future research include studying the effects of autocorrelation similar to the research in Mousavi and Reynolds (2009) and exploring effects of low count data on the performance of the control chart methods similar to the case study presented in Saniga et al. (2009).

Finally, it would be of interested to the study the performance of the two-sided multinomial CUSUM chart. All the multinomial CUSUM charts in this paper are constructed to detect process deterioration. However, there may be situations when the objective is to detect both process deterioration and process improvement. One possible approach is to employ several multinomial CUSUM charts simultaneously that are designed for detecting shifts in different directions. This approach is analogous to Hawkins' (1991, 1993) use of Healy's (1987) method for monitoring a multivariate normal mean vector.

Appendix A: The Markov Chain Representation

The multinomial CUSUM chart properties can be determined through the use of Markov chains. This Markov chain representation is a generalization of the approach taken by Reynolds and Stoumbos (1999), which is simpler than the analytical approach taken by Steiner et al. (1996a). In order for the Markov chain to be applied correctly, the design of the CUSUM chart

must be in a form which results in a finite number of states (CUSUM statistic values) within the transition matrix of the Markov chain. In the case of the Bernoulli CUSUM chart, Reynolds and Stoumbos (1999) showed that this can be achieved by slightly adjusting the out-of-control value, p_1.

The same approach can be used to develop a Markov chain representation of the multinomial CUSUM chart. However, as the number of proportions being monitored increases above two, the determination of appropriate design values for the out-of-control probabilities, $p_{1,i}$, becomes more difficult. One way to generate an appropriate Markov chain to analyze the multinomial CUSUM chart is to allow the statistic, S_t, to only take integer values. This is possible by adjusting $p_{1,i}$ to a value of $p_{1,i}^*$, which forces L_t to take integer values, namely L_t^*, where

$$L_t^* = a \ln\left(\frac{p_{1,i}^*}{p_{0,i}}\right) \text{ for } X_t = i, i = 1, 2, \dots, k, t = 1, 2, \dots, \tag{A1}$$

where $a > 0$, and $p_{1,i}^*$ is a value close to $p_{1,i}$, $i = 1, 2, \dots, k$. Then Equation (4) becomes

$$S_t^* = \max(0, S_{t-1}^* + L_t^*), t = 1, 2, \dots , \tag{A2}$$

where $S_t^* = 0$ and the CUSUM chart signals when $S_t^* > ah_m$. Since S_t^* can only take on integer values, this becomes equivalent to signaling when $S_t^* > \lfloor ah_m \rfloor$, where $\lfloor \cdot \rfloor$ is the integer floor rounding function. We will refer to upper control limit $\lfloor ah_m \rfloor$ as h_m^*. In order to achieve integer values for L_t^* we not only have to find appropriately adjusted values for $p_{1,i}$, we must also determine one optimal value for a that will satisfy our integer value constraint for all of the adjusted $p_{1,i}$ values. To solve this problem, we propose the use of the following numerical optimization routine:

$$\begin{aligned} &\text{Minimize:} && \|aH_1 - \lfloor aH_1 \rceil, aH_2 - \lfloor aH_2 \rceil, \dots, aH_k - \lfloor aH_k \rceil\| \\ &\text{Subject To:} && \textstyle\sum_{i=1}^{k} p_{1,i}^* = 1 \\ & && C^L p_{1,i} \le p_{1,i}^* \le C^U p_{1,i} \text{ for } i = 1, 2, \dots, k \\ & && a^L \le a \le a^U, \end{aligned} \tag{A3}$$

where $H_i = \ln\left(\frac{p_{1,i}^*}{p_{0,i}}\right)$, $\lfloor \cdot \rceil$ is the integer rounding function, $|| \cdot ||$ is the Euclidean norm of the element, $p_{1,i}^*$ is the adjusted value of $p_{1,i}$, a^L and a^U are lower and upper bounds on a, respectively, and C^L and C^U provide lower and upper percentage bounds for allowable adjustments of $p_{1,i}$, respectively.

To solve Equation (A3), the initial value for $p_{1,i}^{*}$ should be set to the corresponding $p_{1,i}$ value. For any given multinomial CUSUM, there may exist an infinite number of "acceptable" local minimum solutions for developing the Markov chain. In addition, as the value of a increases, the number of states in the Markov chain increases, resulting in higher computational costs in obtaining the chart properties. To deal with the aforementioned issues, we suggest that Equation (A3) be solved sequentially by increasing values of a^{L}, a^{U}, and the initial value of a. After each sequential solution of Equation (A3), the values of aH_i for $i = 1, 2, \ldots, k$ should be checked to determine whether or not they are acceptable (close to being integers). If they are not acceptable, one should continue to the next solution; if they are acceptable, one should stop and obtain values for a and $p_{1,i}^{*}$ for $i = 1, 2, \ldots, k$.

Appendix B: Markov Chain Model Example

The Markov chain representation necessary for analyzing the properties of the multinomial CUSUM chart used in Case 1 of our paper is illustrated through the following example. Table 3.1 presents the Case 1 in-control and out-of-control probabilities. For this analysis we set $C^{L} = 0.99$ and $C^{U} = 1.01$, meaning that the original $p_{1,i}$ values are allowed to change by a maximum of $\pm 1\%$. The initial lower (a^{L}) and upper (a^{U}) bounds of the variable a, are 0 and 10, respectively, and the initial value of a is set at 5. This results in an optimal solution where, $aH_0 \approx -1.999$, $aH_1 \approx .9999$, and $aH_2 \approx 5.0000$. For the purposes of analyzing the Markov chain these values are considered acceptable, as they are essentially integers. The integer values will be referred to as a_0, a_1, and a_3, respectively. The value of a for this case is 5.4952, and the adjusted $p_{1,i}$ values can be found in Table 3.1. The Markov chain design parameters for Case 1 through Case 4 are shown in Table 3.B1.

Table 3.B1. Markov Chain Design Parameters for Case 1, Case 2, Case 3, and Case 4

	Case 1	Case 2	Case 3	Case 4
h_m	2.9512	2.8023	0.8337	3.249
a	5.4952	128.4680	107.9466	18.1637
h_m^*	16	359	89	59
a_0	-2	-13	-1	-9
a_1	1	88	74	9
a_2	5	210	179	10
a_3	--	--	--	13

Once the values for H_i and a have been determined, the transition probability matrix, **Q**, of the Markov chain can be generated. For this example, if an observation is in the good category the CUSUM statistic will decrease by -2, in the fair category the CUSUM statistic will increase by 1, and in the bad category the CUSUM statistic will increase by 5. Assuming $p_{i,t} = p_i$ ($i = 1, 2, 3$ and $t = 1, 2, ...$) and $h_m = 2.95$ gives the upper control limit for the Markov chain to be $h_m^* = 16$, resulting in the 16×16 transition probability matrix **Q** being equal to

$$\mathbf{Q} = \begin{array}{c|cccccccc} S_t^* \backslash S_{t+1}^* & 0 & 1 & \cdots & 5 & \cdots & 13 & \cdots & 15 \\ \hline 0 & p_1 & p_3 & & p_2 & & & & \\ \vdots & \vdots & & \ddots & & \ddots & & & \\ 2 & p_1 & & & \ddots & & \ddots & & \\ \vdots & & \ddots & & & \ddots & & \ddots & \\ 10 & & & \ddots & & & \ddots & & p_2 \\ \vdots & & & & \ddots & & & \ddots & \\ 14 & & & & & \ddots & & & p_3 \\ 15 & & & & & & p_1 & & \end{array}, \qquad \text{(B1)}$$

where all elements not identified otherwise are zero. Using the well known equation, we have

$$\mathbf{Z} = \left[\mathrm{z_j}\right]^{\mathrm{T}} = (\mathbf{I} - \mathbf{Q})^{-1}\mathbf{1} \text{ for j} = 0, \ldots, h_m^*, \quad (12)$$

where z_j is the average time until absorption (signal) starting in state j, **I** is the identity matrix, and **1** is a vector of ones. Since the CUSUM statistic starts off at zero $(j = 0)$, the average run length from our Markov chain representation is z_0.

Appendix C: Additional Comparisons for Trinomial Processes

The zero-state ARL performance for three additional trinomial processes is compared, where the three cases are named Case I, Case II, and Case III. Each chart has an in-control ARL of approximately 280 and the simultaneous Bernoulli CUSUM chart ARL values were estimated using 100,000 simulations. The Markov chain formulation was used to calculate ARL values for the multinomial CUSUM chart.

The category probabilities for Case I are displayed in Table 3.C1. The probabilities for good, fair, and bad components are all very close, which is different from any other cases we have studied. The zero-state ARL performance for Case I is given in Table 3.C2. When the category probabilities are very similar, the 2-Bernoulli CUSUM chart that focuses on good and fair components performs well for small parameter shifts. As the shifts become larger and closer to the shift the multinomial CUSUM chart is designed to detect, the multinomial CUSUM has better performance.

Table 3.C1. Probabilities for Case I

Categories	Good (1)	Fair (2)	Bad (3)
In-Control	0.45	0.35	0.20
Out-of-Control	0.25	0.45	0.30
Adjusted Out-of-Control	0.2478	0.4475	0.3047

Table 3.C2. Zero-State ARL Comparisons for Case I

Distribution	p_1 P(Good)	p_2 P(Fair)	p_3 P(Bad)	Multinomial CUSUM ARL $h_m = 3.07$	2-Bernoulli CUSUM ARL $h_g = 3.57$ $h_b = 2.62$	2-Bernoulli CUSUM ARL $h_f = 2.50$ $h_b = 2.785$	2-Bernoulli CUSUM ARL $h_g = 3.5057$ $h_f = 2.3057$	3-Bernoulli CUSUM ARL $h_g = 3.885$ $h_f = 2.645$ $h_b = 2.875$
1 (in-control)	0.45	0.35	0.20	280.49	279.99	281.00	279.37	280.71
2	0.425	0.37	0.205	189.92	201.95	195.13	*177.37*	189.35
3	0.40	0.40	0.20	140.32	157.67	135.15	*111.69*	129.28
4	0.35	0.43	0.22	73.27	81.14	82.80	*66.62*	75.04
5	0.30	0.44	0.26	*42.08*	46.65	58.99	46.12	49.37
6	**0.2478**	**0.4475**	**0.3047**	***27.55***	**31.01**	**43.20**	**32.43**	**33.95**
7	0.20	0.50	0.30	*21.57*	24.63	35.82	24.28	26.59
8	0.15	0.53	0.32	*17.06*	19.62	29.87	19.45	21.26
9	0.10	0.55	0.35	*13.94*	16.12	25.61	16.19	17.60
10	0.05	0.57	0.38	*11.78*	13.72	22.41	13.83	14.91

The category probabilities for Case II are given in Table 3.C3. In this case, the majority of the components produced are good. Table 3.C4 gives the zero-state ARL performance for Case II. Similar to the results for Cases 1 and 2, the multinomial CUSUM chart detects parameter shifts faster than any of the other control charting methods for most shifts studied. The 2-Bernoulli CUSUM chart that focuses on good and bad components has the best ARL performance for small shifts compared to the other simultaneous Bernoulli CUSUM charts and the 2-Bernoulli CUSUM chart that focuses on good and fair components has the best performance for large parameter shifts.

Table 3.C3. Probabilities for Case II

Categories	Good (1)	Fair (2)	Bad (3)
In-Control	0.80	0.15	0.05
Out-of-Control	0.65	0.25	0.10
Adjusted Out-of-Control	0.6479	0.2475	0.1046

Table 3.C4. Zero-State ARL Comparisons for Case II

Distribution	p_1 P(Good)	p_2 P(Fair)	p_3 P(Bad)	Multinomial CUSUM ARL $h_m = 2.67$	2-Bernoulli CUSUM ARL $h_g = 3.133$ $h_b = 2.268$	2-Bernoulli CUSUM ARL $h_f = 2.744$ $h_b = 2.384$	2-Bernoulli CUSUM ARL $h_g = 2.97$ $h_f = 2.47$	3-Bernoulli CUSUM ARL $h_g = 3.347$ $h_f = 2.807$ $h_b = 2.447$
1 (in-control)	0.80	0.15	0.05	285.57	284.17	284.27	284.16	279.99
2	0.775	0.165	0.06	163.11	*159.51*	165.30	168.11	160.33
3	0.75	0.18	0.07	*102.08*	102.13	108.40	109.64	104.03
4	0.72	0.20	0.08	*66.19*	68.49	74.25	71.15	70.06
5	0.705	0.21	0.085	*55.77*	57.83	63.29	59.42	59.33
6	0.69	0.22	0.09	*47.00*	50.01	55.33	50.90	51.52
7	**0.6479**	**0.2475**	**0.1046**	***32.37***	**35.19**	**40.27**	**35.14**	**36.73**
8	0.61	0.27	0.12	*24.84*	27.44	31.98	27.23	28.80
9	0.56	0.30	0.14	*18.89*	21.17	25.24	20.78	22.29
10	0.51	0.33	0.16	*15.19*	17.18	20.80	16.81	18.13
11	0.43	0.39	0.18	*11.68*	13.31	16.36	12.76	14.03
12	0.39	0.41	0.20	*10.37*	11.89	14.75	11.41	12.57
13	0.34	0.44	0.22	*9.13*	10.52	13.14	10.06	11.11
14	0.22	0.52	0.26	*7.09*	8.19	10.50	7.90	8.67
15	0.09	0.60	0.31	*5.68*	6.62	8.63	6.52	6.90

The category probabilities for Case III, given in Table 3.C5, are similar to the probabilities studied in Case I with the probability of good components being slightly larger for Case III. Table 3.C6 gives the zero-state ARL performance for Case III. The multinomial CUSUM chart continues to be the best chart for detecting parameter shifts quickly when the parameter shifts are in the direction in which the chart was designed to detect. Similar to Case II, the 2-Bernoulli CUSUM chart that focuses on good and bad components has the best ARL performance for small shifts compared to the other simultaneous Bernoulli CUSUM charts and the 2-Bernoulli CUSUM chart that focuses on good and fair components has the best performance for large parameter shifts. The overall conclusions involving the zero-state ARL performance for Cases I through III are the same as the conclusions for Cases 1 through 3. Appendix D gives steady-state ARL performance for Cases I through III.

Table 3.C5. Probabilities for Case III

Categories	Good (1)	Fair (2)	Bad (3)
In-Control	0.55	0.30	0.15
Out-of-Control	0.45	0.35	0.20
Adjusted Out-of-Control	0.4481	0.3467	0.2052

Table 3.C6. Zero-State ARL Comparisons for Case III

Distribution	p_1 P(Good)	p_2 P(Fair)	p_3 P(Bad)	Multinomial CUSUM ARL $h_m = 2.05$	2-Bernoulli CUSUM ARL $h_g = 2.49$ $h_b = 1.79$	2-Bernoulli CUSUM ARL $h_f = 1.585$ $h_b = 2.015$	2-Bernoulli CUSUM ARL $h_g = 2.07$ $h_f = 1.60$	3-Bernoulli CUSUM ARL $h_g = 2.635$ $h_f = 1.645$ $h_b = 2.135$
1 (in-control)	0.55	0.30	0.15	279.43	276.33	278.07	278.87	280.36
2	0.53	0.31	0.16	*188.12*	190.52	200.57	193.98	196.11
3	0.51	0.32	0.17	*133.63*	139.27	151.83	142.03	145.98
4	0.49	0.33	0.18	*99.58*	106.13	119.48	107.57	112.22
5	0.47	0.34	0.19	*77.34*	83.73	97.72	84.26	89.43
6	**0.4481**	**0.3467**	**0.2052**	***59.85***	**66.09**	**79.50**	**67.31**	**71.43**
7	0.40	0.38	0.22	*41.19*	47.15	59.17	44.59	50.03
8	0.33	0.42	0.25	*27.25*	32.14	42.35	29.37	33.69
9	0.22	0.48	0.30	*17.56*	21.19	29.29	18.95	21.96
10	0.12	0.53	0.35	*13.17*	16.10	22.69	14.26	16.62
11	0.08	0.55	0.37	*11.97*	14.69	20.81	12.98	15.13
12	0.02	0.58	0.40	*10.54*	12.99	18.53	11.44	13.37

Appendix D: Steady-State ARL Analysis for Cases 1-3

The steady-state ARL comparisons for Cases 1 through 3 and Cases I through III are given in Tables 3.D1 through 3.D6. The ARL values for all cases were estimated using 100,000 simulations except Case 3 where 1 million simulations were used. For all cases, the control limits from the zero-state analyses were used. The process was run in the in-control state for 50 samples and then the shift in the distribution occurred. If a simulated chart signaled the

distribution had shifted during the first samples, then that particular run was discarded and a new set of 50 samples were generated. The multinomial steady-state ARL values were also estimated using simulation instead of the Markov chain formulation.

Through these comparisons, it does not appear that steady-state ARL analyses differ substantially from the zero-state ARL analyses. However, we do notice from the steady-state analyses that multinomial CUSUM chart is not always the best performing chart for small parameter shifts. In Table 3.D1, the 2-Bernoulli CUSUM chart that focuses on good and bad components has better performance than the multinomial CUSUM chart for the first two distribution shifts. The multinomial CUSUM chart is, however, still the best performing chart for the majority of the parameter shifts especially shifts close to the shift the multinomial CUSUM chart was designed to detect. A similar pattern appears in the steady-state analyses for the other cases.

Table 3.D1. Steady-State ARL Comparisons for Case 1

Distribution	p_1 P(Good)	p_2 P(Fair)	p_3 P(Bad)	Multinomial CUSUM ARL $h_m = 2.95$	2-Bernoulli CUSUM ARL $h_g = 3.72$ $h_b = 3.10$	2-Bernoulli CUSUM ARL $h_f = 1.712$ $h_b = 3.332$	2-Bernoulli CUSUM ARL $h_g = 2.93$ $h_f = 2.71$	3-Bernoulli CUSUM ARL $h_g = 3.706$ $h_f = 1.7896$ $h_b = 3.506$
1 (in-control)	0.65	0.25	0.10	280.63	282.38	280.48	280.07	281.00
2	0.625	0.255	0.12	147.41	*145.86*	156.41	169.03	154.86
3	0.60	0.26	0.14	89.99	*89.21*	101.51	113.45	99.02
4	0.55	0.27	0.18	*43.99*	44.34	51.94	58.74	49.63
5	0.50	0.28	0.22	*26.66*	27.57	32.62	35.86	30.71
6	**0.4517**	**0.2999**	**0.2484**	***19.53***	**20.79**	**24.73**	**24.78**	**22.86**
7	0.35	0.35	0.30	*12.55*	13.70	16.79	14.47	14.79
8	0.25	0.40	0.35	*9.18*	10.23	12.75	10.12	10.89
9	0.15	0.45	0.40	*7.20*	8.13	10.25	7.77	8.58
10	0.05	0.50	0.45	*5.95*	6.74	8.58	6.30	7.13

Table 3.D2. Steady-State ARL Comparisons for Case 2

Distribution	p_1 P(Good)	p_2 P(Fair)	p_3 P(Bad)	Multinomial CUSUM ARL $h_m = 2.80$	2-Bernoulli CUSUM ARL $h_g = 3.375$ $h_b = 2.8295$	2-Bernoulli CUSUM ARL $h_f = 2.734$ $h_b = 2.9055$	2-Bernoulli CUSUM ARL $h_g = 3.12$ $h_f = 2.36$	3-Bernoulli CUSUM ARL $h_g = 3.6288$ $h_f = 2.8288$ $h_b = 2.9288$
1 (in-control)	0.94	0.05	0.01	504.40	502.88	501.23	499.20	505.39
2	0.925	0.06	0.015	223.34	*222.83*	222.97	237.57	221.91
3	0.89	0.08	0.03	*70.61*	72.34	76.33	85.14	74.41
4	0.87	0.09	0.04	*46.78*	48.36	52.33	57.89	50.63
5	**0.8495**	**0.0992**	**0.0513**	***33.80***	**35.31**	**38.67**	**42.90**	**37.17**
6	0.80	0.15	0.05	*24.30*	24.71	27.37	24.88	25.80
7	0.74	0.20	0.06	16.70	16.93	19.03	*16.44*	17.70
8	0.60	0.30	0.10	*9.12*	9.51	10.89	9.31	10.01
9	0.50	0.35	0.15	*6.61*	7.05	8.14	7.16	7.47
10	0.40	0.40	0.20	*5.18*	5.58	6.48	5.81	5.94

Table 3.D3. Steady-State ARL Comparisons for Case 3

Distribution	p_1 P(Good)	p_2 P(Fair)	p_3 P(Bad)	Multinomial CUSUM ARL $h_m = 0.8337$	2-Bernoulli CUSUM ARL $h_g = 1.335$ $h_b = 0.0032$	2-Bernoulli CUSUM ARL $h_f = 1.13$ $h_b = 0.004$	2-Bernoulli CUSUM ARL $h_g = 0.928$ $h_f = 0.865$	3-Bernoulli CUSUM ARL $h_g = 1.60$ $h_f = 1.13$ $h_b = 1.38$
1 (in-control)	0.994	0.005	0.001	502.10	498.29	499.94	526.70	499.94
2	0.99	0.0075	0.0025	220.93	*219.44*	220.56	235.29	220.56
3	0.987	0.009	0.004	149.78	*149.09*	150.31	165.83	150.31
4	**0.9848**	**0.0099**	**0.0053**	**120.35**	***119.83***	**121.12**	**136.01**	**121.12**
5	0.98	0.015	0.005	93.87	*93.51*	94.83	96.59	94.83
6	0.974	0.02	0.006	69.81	*69.68*	70.96	71.33	70.96
7	0.96	0.03	0.01	*42.39*	42.40	43.26	44.82	43.26
8	0.95	0.035	0.015	*32.29*	32.33	32.88	35.56	32.88
9	0.94	0.04	0.02	*26.15*	26.18	26.58	29.56	26.58
10	0.9	0.06	0.04	*14.88*	14.90	15.03	17.69	15.03
11	0.85	0.09	0.06	*9.89*	9.90	9.98	11.79	9.98
12	0.8	0.11	0.09	7.21	*7.20*	7.25	8.85	7.25
13	0.7	0.17	0.13	*4.84*	*4.84*	4.87	5.89	4.87
14	0.6	0.24	0.16	3.70	*3.69*	3.71	4.42	3.71
15	0.5	0.3	0.2	*2.96*	*2.96*	2.97	3.54	2.97
16	0.3	0.4	0.3	*2.08*	*2.08*	2.09	2.53	2.09

Table 3.D4. Steady-State ARL Comparisons for Case I

Distribution	p_1 P(Good)	p_2 P(Fair)	p_3 P(Bad)	Multinomial CUSUM ARL $h_m = 3.07$	2-Bernoulli CUSUM ARL $h_g = 3.57$ $h_b = 2.62$	2-Bernoulli CUSUM ARL $h_f = 2.50$ $h_b = 2.785$	2-Bernoulli CUSUM ARL $h_g = 3.5057$ $h_f = 2.3057$	3-Bernoulli CUSUM ARL $h_g = 3.885$ $h_f = 2.645$ $h_b = 2.875$
1 (in-control)	0.45	0.35	0.20	280.49	279.99	281.00	279.37	280.71
2	0.425	0.37	0.205	179.54	185.80	171.73	*160.80*	168.07
3	0.40	0.40	0.20	130.14	143.70	115.27	*97.89*	111.67
4	0.35	0.43	0.22	65.93	71.46	68.16	*56.94*	62.45
5	0.30	0.44	0.26	*37.12*	39.98	47.30	38.80	40.58
6	**0.2478**	**0.4475**	**0.3047**	***23.63***	**25.73**	**33.85**	**26.86**	**27.50**
7	0.20	0.50	0.30	*18.18*	20.18	27.49	19.77	21.35
8	0.15	0.53	0.32	*14.14*	15.91	22.66	15.58	16.93
9	0.10	0.55	0.35	*11.41*	12.94	19.20	12.90	13.96
10	0.05	0.57	0.38	*9.54*	10.91	16.68	10.97	11.80

Table 3.D5. Steady-State ARL Comparisons for Case II

Distribution	p_1 P(Good)	p_2 P(Fair)	p_3 P(Bad)	Multinomial CUSUM ARL $h_m = 2.67$	2-Bernoulli CUSUM ARL $h_g = 3.133$ $h_b = 2.268$	2-Bernoulli CUSUM ARL $h_f = 2.744$ $h_b = 2.384$	2-Bernoulli CUSUM ARL $h_g = 2.97$ $h_f = 2.47$	3-Bernoulli CUSUM ARL $h_g = 3.347$ $h_f = 2.807$ $h_b = 2.447$
1 (in-control)	0.80	0.15	0.05	285.57	284.17	284.27	284.16	279.99
2	0.775	0.165	0.06	150.72	146.83	148.68	156.59	*144.76*
3	0.75	0.18	0.07	92.99	92.00	95.15	99.50	*91.79*
4	0.72	0.20	0.08	*59.99*	60.71	63.62	63.96	60.56
5	0.705	0.21	0.085	*49.46*	51.15	54.09	53.06	51.46
6	0.69	0.22	0.09	*42.18*	43.79	46.81	45.10	43.97
7	**0.6479**	**0.2475**	**0.1046**	***28.40***	**30.33**	**33.31**	**30.75**	**30.87**
8	0.61	0.27	0.12	*21.51*	23.23	26.12	23.48	24.00
9	0.56	0.30	0.14	*16.26*	17.72	20.36	17.72	18.42
10	0.51	0.33	0.16	*12.92*	14.25	16.65	14.18	14.86
11	0.43	0.39	0.18	*9.84*	10.95	13.04	10.66	11.44
12	0.39	0.41	0.20	*8.72*	9.76	11.66	9.50	10.22
13	0.34	0.44	0.22	*7.67*	8.59	10.33	8.34	9.02
14	0.22	0.52	0.26	*5.93*	6.68	8.17	6.51	7.02
15	0.09	0.60	0.31	*4.75*	5.38	6.69	5.27	5.62

Table 3.D6. Steady-State ARL Comparisons for Case III

Distribution	p_1 P(Good)	p_2 P(Fair)	p_3 P(Bad)	Multinomial CUSUM ARL $h_m = 2.05$	2-Bernoulli CUSUM ARL $h_g = 2.49$ $h_b = 1.79$	2-Bernoulli CUSUM ARL $h_f = 1.585$ $h_b = 2.015$	2-Bernoulli CUSUM ARL $h_g = 2.07$ $h_f = 1.60$	3-Bernoulli CUSUM ARL $h_g = 2.635$ $h_f = 1.645$ $h_b = 2.135$
1 (in-control)	0.55	0.30	0.15	279.43	276.33	278.07	278.87	280.36
2	0.53	0.31	0.16	171.54	*168.65*	170.76	172.34	168.68
3	0.51	0.32	0.17	*119.61*	120.31	126.00	123.33	122.67
4	0.49	0.33	0.18	*87.40*	89.74	97.19	92.17	92.70
5	0.47	0.34	0.19	*66.95*	70.12	78.44	71.17	72.81
6	**0.4481**	**0.3467**	**0.2052**	***51.17***	**54.27**	**63.01**	**56.20**	**57.55**
7	0.40	0.38	0.22	*34.06*	37.94	45.50	36.28	39.61
8	0.33	0.42	0.25	*22.05*	25.13	31.66	23.38	26.08
9	0.22	0.48	0.30	*13.78*	16.19	21.33	14.69	16.75
10	0.12	0.53	0.35	*10.21*	12.16	16.48	10.95	12.60
11	0.08	0.55	0.37	*9.28*	11.08	15.16	9.96	11.44
12	0.02	0.58	0.40	*8.11*	9.75	13.41	8.73	10.09

Acknowledgments

This research was partially supported by NSF grant CMMI-0927323. The authors appreciate the helpful comments from the Editor and two anonymous reviewers.

References

Duncan, A. J. (1950). "A Chi-Square Chart for Controlling a Set of Percentages". *Industrial Quality Control* 7, pp. 11-15.

Gan, F. F. (1993). "An Optimal Design of CUSUM Control Charts for Binomial Counts". *Journal of Applied Statistics* 20, pp. 445-460.

Hawkins, D. M. (1991). "Multivariate Quality Control Based on Regression-Adjusted Variables". *Technometrics* 33, pp. 61-75.

Hawkins, D. M. (1993). "Regression Adjustment for Variables in Multivariate Quality Control". *Journal of Quality Technology* 25, pp. 170-182.

Healy, J. D. (1987). "A Note on Multivariate CUSUM Procedures". *Technometrics* 29, pp. 409-412.

Marcucci, M. (1985). "Monitoring Multinomial Processes". *Journal of Quality Technology* 17, pp. 86-91.

Mousavi, S. and Reynolds, M. R., Jr. (2009). "A CUSUM Chart for Monitoring a Proportion with Autocorrelated Binary Observations". *Journal of Quality Technology* 41, pp. 401-414.

Nelson, L. S. (1987). "A Chi-Square Control Chart for Several Proportions". *Journal of Quality Technology* 19, pp. 229-231.

Reynolds, M. R., Jr. and Stoumbos, Z. G. (1999). "A CUSUM Chart for Monitoring a Proportion When Inspecting Continuously". *Journal of Quality Technology* 31, pp. 87-108.

Saniga, E. M.; Davis, D. J.; and Lucas, J. M. (2009). "Using Shewhart and CUSUM Charts for Diagnosis with Count Data in a Vendor Certification Study". *Journal of Quality Technology* 41, pp. 217-227.

Steiner, S. H. (1998). "Grouped Data Exponentially Weighted Moving Average Control Charts". *Journal of the Royal Statistical Society. Series C (Applied Statistics)* 47, pp. 203-316.

Steiner, S. H.; Cook, R. J.; Farewell, V. T.; and Treasure, T. (2000). "Monitoring Surgical Performance Using Risk-Adjusted Cumulative Sum Charts". *Biostatistics* 1, pp. 441-452.

Steiner, S. H.; Geyer, P. L.; and Wesolowsky, G. O. (1994). "Control Charts Based on Grouped Observations". *International Journal of Production Research* 32, pp. 75-91.

Steiner, S. H.; Geyer, P. L.; and Wesolowsky, G. O. (1996a). "Grouped Data Sequential Probability Ratio Tests and Cumulative Sum Control Charts". *Technometrics* 38, pp. 230-237.

Steiner, S. H.; Geyer, P. L.; and Wesolowsky, G. O. (1996b). "Shewhart Control Charts to Detect Mean and Standard Deviation Shifts Based on Grouped Data". *Quality and Reliability Engineering International* 12, pp. 345-353**.**

Topalidou, E. and Psarakis, S. (2009). "Review of Multinomial and Multiattribute Quality Control Charts". *Quality and Reliability Engineering International* 25, pp. 773-804.

Tucker, G. R.; Woodall, W. H.; and Tsui, K. L. (2002). "A Control Chart Method for Ordinal Data". *American Journal of Mathematical and Management Sciences* 22, pp. 31-48.

Woodall, W. H. (1997). "Control Charts Based on Attribute Data: Bibliography and Review". *Journal of Quality Technology* 29, pp. 172-183.

Chapter 4

Conclusions and Future Work

Control charting methods prove to be important tools in both industrial quality control and public health surveillance. The best performing control chart should be chosen for the situation at hand. In the Poisson case where the area of opportunity varies, comparisons reveal that the GLR CUSUM chart based on the likelihood-ratio formulation performs best for the shift in which the chart was designed to detect and also has the quickest detection for many shifts around the shift of interest.

The modified EWMA-M method with the reflecting lower barrier and control limits based on the exact variances of the EWMA statistics also performs well for many different shifts as long as the smoothing constant is chosen based on the size of the shift one is interested in detecting. In Dong et al. (2008) the EWMA chart with $r = .9$ was recommended to detect shifts in a Poisson process where the sample size varies. Our comparisons reveal that this chart with the high smoothing constant will only perform well when the shift of interest is very large. The chart, however, has poor performance when the objective is to detect small shifts quickly. In situations where the objective is to detect large shifts quickly, it may be beneficial to use a simple Shewhart chart rather than an EWMA chart with such a high smoothing constant.

In our research, we assume that the in-control Poisson rate, λ_0, is estimated without error and we assume the Poisson count data are independent observations. The effects of estimation error on the performance of the different control chart methods along with the effects of autocorrelation are areas for future research.

In the multinomial case, the multinomial CUSUM chart based on the likelihood-ratio formulation has nice ARL properties when the category probabilities shift in the direction in which the multinomial CUSUM chart was designed to detect. For most parameter shifts the multinomial CUSUM chart is the best performing chart especially for parameter shifts that are close to the shift in which the chart was designed to detect.

When we began our research regarding control charting methods for multinomial data, we assumed that the different $k-1$ simulatenous Bernoulli CUSUM charts would perform similarly and there would be no need to monitor with the k-Bernoulli CUSUM chart since the category probabilities must sum to one. Our simulation studies led to different conclusions. The selection of the categories to monitor when using the $k-1$ simultaneous Bernoulli CUSUM charts has a significant impact on the performance of the chart. The performance of the k-Bernoulli CUSUM chart also differs from the performance of the $k-1$ simultaneous Bernoulli CUSUM charts. In situations where the objective is to detect shifts in any direction, then we recommend using the k-Bernoulli CUSUM chart as opposed to selecting one of the $k-1$ simultaneous Bernoulli CUSUM charts because of the difficulty associated with selecting the best performing $k-1$ simultaneous Bernoulli CUSUM chart without performing a simulation study. Also, the k-Bernoulli CUSUM chart avoids some of the worst ARL performance that is associated with various simultaneous Bernoulli CUSUM charts and the multinomial CUSUM chart. Determination of further guidelines for the choice of the best performing Bernoulli CUSUM charts for multinomial processes is an objective for future studies.

Another area of future research would be to construct a risk-adjusted multinomial CUSUM chart similar to Steiner et al.'s (2000) risk-adjusted Bernoulli CUSUM chart. Risk-adjustment is essential in many areas of public health surveillance and the multinomial CUSUM chart could be adapted to incorporate risk adjustment.

Finally, it would also be of interest to study the properties of a two-sided multinomial CUSUM chart. The research thus far has focused on the one-sided multinomial CUSUM chart where the only objective is to detect changes in the categories in a single specified direction. The two-sided multinomial CUSUM chart would allow for detection of process improvement as well as process deterioration. More generally, several multinomial CUSUM charts could be employed simultaneously, each designed for detection of shifts in different directions. This is analogous to

Hawkins' (1991, 1993) use of Healy's (1987) method in the case of monitoring a multivariate normal mean vector.

References

(Not included in Chapter 2 or Chapter 3)

Page, E. S. (1954). “Continuous Inspection Schemes”. *Biometrics* 41, pp. 100-115.

Roberts, S. W. (1959). “Control Chart Tests Based on Geometric Moving Averages”. *Technometrics* 42, pp. 97-102.

Ryan, A. G.; Wells, L. J.; and Woodall, W. H. (2011). “Methods for Monitoring Multiple Proportions When Inspecting Continuously". To appear in *Journal of Quality Technology*.

Ryan, A. G. and Woodall, W. H. (2010). “Control Charts for Poisson Count Data with Varying Samples Sizes”. *Journal of Quality Technology* 42, pp. 260-275.

Shewhart, W. A. (1939). *Statistical Method from the Viewpoint of Quality Control*. The Graduate School, the Department of Agriculture, Washington, D.C.